Environ Fluid Mech
DOI 10.1007/s10652-008-9117-0

ORIGINAL ARTICLE

Energy conservation and second-order statistics in stably stratified turbulent boundary layers

Victor S. L'vov · Itamar Procaccia · Oleksii Rudenko

Received: 28 June 2007 / Accepted: 27 November 2008

Abstract We address the dynamical and statistical description of stably stratified turbulent boundary layers with the important example of the atmospheric boundary layer with a stable temperature stratification in mind. Traditional approaches to this problem, based on the profiles of mean quantities, velocity second-order correlations, and dimensional estimates of the turbulent thermal flux run into a well-known difficulty, predicting the suppression of turbulence at a small critical value of the Richardson number, in contradiction with observations. Phenomenological attempts to overcome this problem suffer from various theoretical inconsistencies. Here we present a closure approach taking into full account all the second-order statistics, which allows us to respect the conservation of total mechanical energy. The analysis culminates in an analytic solution of the profiles of all mean quantities and all second-order correlations removing the unphysical predictions of previous theories. We propose that the approach taken here is sufficient to describe the lower parts of the atmospheric boundary layer, as long as the Richardson number does not exceed an order of unity. For much higher Richardson numbers the physics may change qualitatively, requiring careful consideration of the potential Kelvin-Helmoholtz waves and their interaction with the vortical turbulence.

Keywords Atmospheric boundary layer · Stable stratification · Richardson number · Transport equations · Second order closure · Algebraic model

V. S. L'vov · I. Procaccia · O. Rudenko (✉)
Department of Chemical Physics, The Weizmann Institute of Science, Rehovot 76100, Israel
e-mail: oleksii.rudenko@weizmann.ac.il

V. S. L'vov
e-mail: victor.lvov@weizmann.ac.il

I. Procaccia
e-mail: itamar.procaccia@weizmann.ac.il

Published online: 19 December 2008

Nomenclature

$\boldsymbol{\mathcal{A}}$	Thermal flux production vector, (19e)
$\boldsymbol{\mathcal{B}}$	Pressure-temperature-gradient-vector, (19f)
$\mathcal{C}_{ij}$	Energy conversion tensor, (19b)
$\mathcal{D}/\mathcal{D}t$	Substantial derivative, $\partial/\partial t + \boldsymbol{\mathcal{U}} \cdot \boldsymbol{\nabla}$
D/Dt	Mean substantial derivative, $\partial/\partial t + \boldsymbol{U} \cdot \boldsymbol{\nabla}$
E_{K}	Turbulent kinetic energy per unit mass, $\langle \boldsymbol{u}^2 \rangle/2$
E_{Θ}	"Temperature energy" per unit mass, $\langle \theta^2 \rangle/2$
$\boldsymbol{F}$	Turbulent thermal flux per unit mass, $\langle \boldsymbol{u}\theta \rangle$
F_*	Thermal flux at zero elevation $z = 0$
$\boldsymbol{g}$	Gravity acceleration, $\boldsymbol{g} = -g\,\widehat{\boldsymbol{z}}$
L	Monin-Obukhov length, $u_*^3/\beta F_*$
$\ell(z)$	Outer scale of turbulence, external parameter
$\mathcal{P}_{ij}$	Rate of Reynolds stress production, (19a)
p, $\widetilde{p}$, p_*	Total, fluctuating and zero level pressures
Pr_{T}	Turbulent Prandtl number, $\nu_{\mathrm{T}}/\chi_{\mathrm{T}}$
$\mathrm{Ri}_{\mathrm{flux}}$	Flux Richardson number, $\beta F_z/\tau_{xz} S_{\mathrm{U}}$
$\mathrm{Ri}_{\mathrm{grad}}$	Gradient Richardson number, $\beta S_{\Theta}/S_{\mathrm{U}}^2$
$\mathcal{R}_{ij}$	Pressure-rate-of-strain-tensor, (19c)
S_{U}	Mean velocity gradient, dU/dz
S_{Θ}	Mean potential temperature gradient, $d\Theta/dz$
T, T_*	Molecular temperature, molecular temperature at zero level
$\boldsymbol{\mathcal{U}}$, $\boldsymbol{U}$, $\boldsymbol{u}$	Total, mean, $\langle \boldsymbol{\mathcal{U}} \rangle$, and fluctuating, $\boldsymbol{\mathcal{U}} - \boldsymbol{U}$, velocity fields
u_*	(Wall) friction velocity, $\sqrt{\tau_*}$
$\widehat{\mathbf{x}}$, $\widehat{\mathbf{z}}$	Horizontal (streamwise) and vertical (wall-normal) unit vectors
β	Buoyancy parameter, $\boldsymbol{g}\widetilde{\beta}$ (for an ideal gas $\boldsymbol{g}/T_{\mathrm{b}}$)
$\widetilde{\beta}$	Thermal expansion coefficient, $-\left(\partial\rho_{\mathrm{b}}/\partial T_{\mathrm{b}}\right)_p/\rho_{\mathrm{b}}$
γ_{RI}	Relaxation frequency of τ_{ij}, $i = j$
$\widetilde{\gamma}_{\mathrm{RI}}$	Relaxation frequency of τ_{ij}, $i \neq j$
γ_{RD}	Relaxation frequency of $\boldsymbol{F}$
γ_{uu}	Relaxation frequency of E_{K}
$\gamma_{\theta\theta}$	Relaxation frequency of E_{Θ}
ε_{ij}	Dissipation tensor of τ_{ij}, (18)
$\boldsymbol{\varepsilon}$	Dissipation vector of $\boldsymbol{F}$, (18)
ε	Dissipation of E_{Θ}, (18)
$\overline{\Theta}$	Potential temperature, (8)
Θ_d	Deviation of potential temperature from BRS, $\overline{\Theta} - T_*$
Θ, θ	Mean, $\langle \Theta_d \rangle$, and fluctuating, $\Theta_d - \langle \Theta_d \rangle$, parts of Θ_d
θ_*	Potential temperature at zero elevation, F_*/u_*
$\Lambda(z)$	Local Monin-Obukhov length, $\tau_{xz}\sqrt{-\tau_{xz}}\,\big/\beta F_z$
λ_*	Viscous lengthscale, ν/u_*
ν, ν_{T}	Kinematic and turbulent viscosity
ρ, ρ_{b}	Total and BRS density of the fluid
τ_{ij}	Reynolds stress tensor per unit mass, $\langle u_i u_j \rangle$
τ_*	Mechanical momentum flux at zero elevation (at the ground), $\nu S_{\mathrm{U}}(0)$
χ, χ_{T}	Kinematic and turbulent thermal conductivity
BRS	Basic reference state

1 Introduction

The lower levels of the atmosphere are usually strongly influenced by the Earth's surface. Known as the atmospheric boundary layer, this is the part of the atmosphere where the surface influences the temperature, moisture, and velocity of the air above through the turbulent transfer of mass.

The stability of the atmospheric boundary layer depends on the profiles of the density and the temperature as a function of the height above the ground. During normal summer days the land mass warms up and the temperature is higher at lower elevations. If it were not for the decrease in density of the air as a function of the height, such a situation of heating from below would have been always highly unstable. In fact, the boundary layer is considered stable as long as the temperature decreases at the dry adiabatic lapse rate ($-9.8°$C per kilometer) throughout most of the boundary layer. With such a rate of cooling one balances out the decrease in density. With a higher degree of cooling one refers to the atmospheric boundary layer as unstably stratified, whereas with a lower degree of cooling the situation is stably stratified. Stably stratified boundary layer occurs typically during clear, calm nights. In extreme cases turbulence tends to cease, and radiational cooling from the surface results in a temperature that increases with height above the surface.

The tendency of the atmosphere to be turbulent does not depend only on the rate of cooling but also on the mean shear in the vertical direction. The commonly used parameter to describe the tendency of the atmosphere to be turbulent is the "gradient" Richardson number, $\mathrm{Ri}_{\mathrm{grad}}$, which represents the ratio of the generation or suppression of turbulence by buoyant production of energy to the mechanical generation of energy by wind shear.

In this paper we consider the description of stably stratified turbulent boundary layers (TBL), taking as an example the case of stable thermal stratification. Since the 50's of twentieth century, traditional models of stratified TBL generalize models of unstratified TBL, based on the budget equations for the kinetic energy and mechanical momentum; see reviews [1,2]. The main difficulty is that the budget equations are not closed; they involve turbulent fluxes of mechanical moments τ_{ij} (known as the "Reynolds stress" tensor) and a thermal flux $\boldsymbol{F}$ (for the case of thermal stratification):

$$\tau_{ij} \equiv \langle u_i u_j \rangle, \quad \boldsymbol{F} \equiv \langle \boldsymbol{u}\theta \rangle, \tag{1}$$

where $\boldsymbol{u}$ and θ stand for the turbulent fluctuating velocity and the potential temperature with zero mean. The nature of the averaging procedure behind the symbol $\langle \cdots \rangle$ will be specified below.

Earlier estimates of the fluxes (1) are based on the concept of the down-gradient turbulent transport, in which, similarly to the case of molecular transport, a flux is taken proportional to the gradient of transported property times a corresponding (turbulent) transport coefficient:

$$\tau_{xz} = -\nu_{\mathrm{T}}\, dU_x \big/ dz, \quad \nu_{\mathrm{T}} \approx C_\nu\, \ell_z \sqrt{\tau_{zz}}, \tag{2a}$$

$$F_z = -\chi_{\mathrm{T}}\, d\Theta \big/ dz, \quad \chi_{\mathrm{T}} \approx C_\chi\, \ell_z \sqrt{\tau_{zz}}, \quad \text{etc.} \tag{2b}$$

Here the turbulent-eddy viscosity ν_{T} and turbulent thermal conductivity χ_{T} are estimated by dimensional reasoning via the vertical turbulent velocity $\sqrt{\tau_{zz}}$ and a scale ℓ_z (which in the simplest case is determined by the elevation z). The dimensionless coefficients C_ν and C_χ are assumed to be of the order of unity.

This approach meets serious difficulties [3], in particular, it predicts full suppression of turbulence when the stratification exceeds a critical level, for which $\mathrm{Ri}_{\mathrm{grad}} = \mathrm{Ri}_{\mathrm{cr}} \approx 0.25$. On the other hand, in observations of the atmospheric turbulent boundary layer the turbulence

exists for much larger values than $\mathrm{Ri}_{\mathrm{grad}} = 0.25$: experimentally above $\mathrm{Ri}_{\mathrm{grad}} = 10$ and even more (see [4,5] and references therein). In models for weather predictions this problem is "fixed" by introducing fit functions $C_\nu(\mathrm{Ri}_{\mathrm{grad}})$ and $C_\chi(\mathrm{Ri}_{\mathrm{grad}})$ instead of the constant C_ν and C_χ in the model parametrization (2) (see reviews [1–3,6], and references therein). This technical "solution" is not based on any physical derivation and just masks the shortcomings of the model. To really solve the problem one has to understand its physical origin, even though from a purely formal viewpoint it is indeed possible that a dimensionless coefficient like C_χ can be any function of $\mathrm{Ri}_{\mathrm{grad}}$.

To expose the physical reason for the failure of the down-gradient approach, recall that in a stratified flow, in the presence of gravity, the turbulent kinetic energy is *not* an integral of motion. Only the total mechanical energy, the sum of the kinetic and the potential energy, is conserved in the inviscid limit. As it was shown already by Richardson [7,8], the difficult point is that an important contribution to the potential energy comes not just from the mean density profile, but from the density fluctuations. Clearly, any reasonable model of the turbulent boundary layer must obey the conservation laws.

The physical requirement of conserving the total mechanical energy calls for an explicit consideration not only of the mean profiles, but also of *all* relevant second-order, one-point, simultaneous correlation functions of *all* the fluctuating fields together with some closure procedure for the appearing third order moments. These fields are the Reynolds stress tensor, $\tau_{ij} = \langle u_i u_j \rangle$, the turbulent potential energy which is proportional to the variance of the potential temperature deviation, $\langle \theta^2 \rangle$, and the thermal flux $\boldsymbol{F} = \langle \boldsymbol{u}\theta \rangle$.

An attempt to improve the modeling of stably stratified flows with the aim to remove $\mathrm{Ri}_{\mathrm{cr}}$ is reported in Ref. [9]. Constructing their second-order scheme, the authors replaced the unwarranted approximation (2b), with an exact equation for the vertical thermal flux F_z and for the "temperature energy" $\langle \theta^2 \rangle /2$, using dimensional reasoning to estimate the required third-order correlations. To account for the important effect of stratification on the anisotropy of turbulence, budget equations for the partial kinetic energies $\tau_{ii}/2$ are explicitly considered in [9]. Nevertheless, the authors of Ref. [9] do not close rigorously the momentum budget equation. They combine three terms in this equations into, what they called "effective dissipation rate", arriving actually again at the down-gradient approximation (2a) for the vertical flux of x-component of the mechanical moment, τ_{xz}. In our paper we treat these three terms separately, considered also explicitly the horizontal heat flux F_x. As a result, we demonstrated, that the down-gradient approximation for the mechanical moment (2a), used in [9], fails in the same manner, as the approximation (2b) for the heat flux.

In this paper we suggest a relatively simple second-order closure model of turbulent boundary layer with stable temperature stratification that, from one hand, accounts for main relevant physics in the stratified TBL and, from the other hand, is simple enough to allow complete analytical treatment including the problem of critical $\mathrm{Ri}_{\mathrm{grad}}$. To reach this goal we approximate the third order correlations via the first- and second-order ones, accounting only for the most physically important terms. Resulting second-order model consist of nine coupled equations for the mean velocity and temperature gradients, four components of the Reynolds stresses, two components of the temperature fluxes and the temperature variance. As a result we found an approximate analytical solution of these equations, expressing all nine correlations as functions of only one governing parameter, $\ell(z)/\Lambda(z)$, where $\ell(z)$ is the outer scale of turbulence (depending on the elevation z and also known as the "dissipation scale") and $\Lambda(z)$—is the local Monin-Obukhov length [10].

It should be noticed that traditional turbulent closures (including ours) cannot be applied for strongly stratified flows with $\mathrm{Ri}_{\mathrm{grad}} \sim 1$ or larger. The main reason is that these closures

are roughly justified for developed *vortical* turbulence, in which the eddy-turnover time is of the order of its life time; in other words, there are no well defined "quasi-particles" or waves. This is not the case for stable stratification with $\mathrm{Ri}_{\mathrm{grad}} \sim 1$ or larger, in which the Brunt-Väisälä frequency

$$N \equiv \sqrt{\beta d\Theta(z)/d\,z}, \tag{3}$$

is larger then the eddy-turnover frequency γ. It means that for $\mathrm{Ri}_{\mathrm{grad}}$ of $\mathcal{O}(1)$ there are weakly decaying Kelvin-Helmoholtz internal gravity waves (with characteristic frequency N and decay time above $1/\gamma$), propagating on large distances, essentially effecting on TBL, as pointed out by [11]. Having in mind that the internal gravity waves significantly change the physics of TBL, we concentrate in our paper on self-consistent description of the lower part of the atmospheric TBL, in which turbulence has vortical character and consequently, large values of $\mathrm{Ri}_{\mathrm{grad}}$ do not appear. We relate large values of $\mathrm{Ri}_{\mathrm{grad}}$ in the upper part of TBL with contributions of the internal gravity waves to the energy and the energy flux in TBL, to the momentum flux, and to the production of (vortical) turbulent energy. Due to their instability in a shear flow, the waves can break and create turbulent kinetic energy. All these effects are beyond the framework of our paper. Their description in the upper "potential-wave" TBL and intermediate region with the combined "vortical-potential" turbulent velocity field is in our nearest agenda.

The paper is organized it as follows.

In Sect. 2.1 we use the Oberbeck-Boussinesq approximation and apply the standard Reynolds decomposition to derive equations for the mean values and balance equations for all relevant second-order correlation functions. In Sect. 2.2 we demonstrate that the resulting balance equations exactly preserve (in the non-dissipative limit) the total mechanical energy of the system, that consists of the kinetic energy of the mean flow, kinetic energy and potential energy of the turbulent subsystem.

In Sect. 3 we describe the proposed closure procedure that results in a model of stably stratified TBL, that accounts explicitly for all relevant second-order correlations. The third order correlations which appear in the theory are modeled in terms of second-order correlations in Sects. 3.1 and 3.2. Further simplifications are presented in Sects. 3.3 and 3.4 for stationary turbulent flows in a plane geometry outside the viscous and buffer layers. In Sect. 3.5 we suggest a generalization of the standard "wall-normalization" to obtain the model equations in a dimensionless form with only one governing parameter, $\ell(z)/\Lambda(z)$.

The last Sect. 4 is devoted to a detailed description of our results (Sect. 4.1): profiles of the mean velocity and potential temperature (Sect. 4.2), profiles of the turbulent kinetic and "temperature" energies, profiles of the anisotropy of partial kinetic energies (Sect. 4.3), profiles of the turbulent transport parameters ν_{T} and χ_{T}, profiles of the gradient- and flux-Richardson numbers $\mathrm{Ri}_{\mathrm{grad}}$ and $\mathrm{Ri}_{\mathrm{flux}}$, and the dependence of the turbulent Prandtl number Pr_{T} versus ℓ/Λ and $\mathrm{Ri}_{\mathrm{grad}}$, Sect. 4.4. The comparison of the model predictions with experimental and LES results are proposed in Sect. 4.4.1. The validity of the down-gradient transport concept (2) and an explanation why it is violated in the upper part of TBL is given in Sect. 4.4.2; the problem of critical $\mathrm{Ri}_{\mathrm{grad}}$ is also discussed there.

2 Simplified dynamics in stably temperature-stratified TBL and its conservation laws

The aim of this section is to consider simplified dynamics of a stably temperature-stratified turbulent boundary layer, aiming finally at an explicit description of the height dependence of important quantities like the mean velocity, mean temperature, turbulent kinetic and potential

energies, etc. In general one expects very different profiles from those known in unstratified wall-bounded turbulence.

2.1 Simplified hydrodynamic equations and Reynolds decomposition

First we briefly overview the derivation of the governing equations in the Boussinesq approximation [12,13]. The system of hydrodynamic equations describing a fluid in which the temperature is not uniform consists of the Navier-Stokes equation for the fluid velocity, $\boldsymbol{\mathcal{U}}(\boldsymbol{r}, t)$, a continuity equation for the space and time dependent (total) density of the fluid, $\rho(\boldsymbol{r}, t)$, and of the heat balance equation for the (total) entropy per unit mass, $\mathcal{S}(\boldsymbol{r}, t)$, [14]:

$$\rho\left(\tfrac{\partial}{\partial t} + \boldsymbol{\mathcal{U}}\cdot\boldsymbol{\nabla}\right)\boldsymbol{\mathcal{U}} = -\boldsymbol{\nabla} p + \boldsymbol{g}\rho + \boldsymbol{\nabla}\cdot\mu\,\boldsymbol{\nabla}\boldsymbol{\mathcal{U}}, \tag{4a}$$

$$\tfrac{\partial \rho}{\partial t} + \boldsymbol{\nabla}\cdot(\rho\boldsymbol{\mathcal{U}}) = 0, \tag{4b}$$

$$\rho\left(\tfrac{\partial}{\partial t} + \boldsymbol{\mathcal{U}}\cdot\boldsymbol{\nabla}\right)\mathcal{S} = \boldsymbol{\nabla}\cdot\kappa\boldsymbol{\nabla}\mathcal{S}. \tag{4c}$$

Here p is pressure, $\boldsymbol{g} = -\widehat{\mathbf{z}}g$ is the vertical acceleration due to gravity, μ and κ are the (molecular) dynamical viscosity and heat conductivity.

Notice, that the role of the Coriolis force, omitted in Eq. 4 is twofold. First, it determines the finite height H_{Z} (Zilitinkevich length [15]) of atmospheric TBL with stable temperature stratification:

$$H_{\mathrm{Z}} \simeq \sqrt{L\lambda}, \quad \lambda \simeq u_*/f. \tag{5}$$

Here λ is the Tennekes height of atmospheric TBL without stratification, u_* is the friction velocity, $f = 2\Omega\sin\varphi$ is the Coriolis parameter expressed via the frequency of the Earth rotation Ω and latitude φ. Second, it leads to a vertical dependence of the mean wind and mean horizontal heat flux parallel to it . As it is shown by Nieuwstadt [10] in the reference system in which on every elevation the x-axis is directed along the mean wind, the resulting model equation with the Coriolis force looks exactly as equation that follows from Eq. 4, but with z-dependent streamwise and spanwise directions. All these allow to use the shortcut in our approach, neglecting the Coriolis force in Eq. 4, having in mind that this does not effect on the resulting profiles of absolute values of the mean shear, horizontal heat flux and other objects of interest, providing that z-dependencies of the vertical mechanical momentum and heat fluxes are prescribed.

Equation 4 are considered with boundary conditions that maintain the solution far from the equilibrium state, where $\boldsymbol{\mathcal{U}} = \mathcal{S} = 0$. These boundary conditions are $\boldsymbol{\mathcal{U}} = 0$ at zero elevation, $\boldsymbol{\mathcal{U}} = \text{const}$ at a high elevation of a few kilometers. This reflects the existence of a wind at high elevation, but we do not attempt to model the physical origin of this wind in any detail. The only important condition with regards to this wind is that it maintains a momentum flux towards the ground that is prescribed as a function of the elevation. Similarly, we assume that a stable temperature stratification is maintained such that the heat flux towards the ground is prescribed as well.

Pressure fluctuations caused by turbulent velocity fluctuations $\boldsymbol{u}$ propagate in a compressible medium with the sound velocity c_{s}, causing time dependent density fluctuations of the order of $(u/c_{\mathrm{s}})^2\langle\rho\rangle$, where $\langle\rho\rangle$ is the mean (in time) density profile, depending on the elevation z. Assuming that the square of the turbulent Mach number $M_{\mathrm{T}}^2 \equiv (u/c_{\mathrm{s}})^2$ is small compared to unity, we can neglect in Eq. 4b the partial time derivative and density fluctuations, see e.g. [14]. Hence, for $M_{\mathrm{T}}^2 \ll 1$

$$\boldsymbol{\nabla}\cdot(\langle\rho\rangle\boldsymbol{\mathcal{U}}) = 0. \tag{6}$$

Even in tropical hurricanes of category five the mean wind velocity U is below 80 m/s. Usually, the turbulent velocity fluctuations u are less then $U/10$, i.e. even in these extreme conditions $u < 8$ m/s and $M_{\mathrm{T}}^2 < 10^{-3}$ (with $c_{\mathrm{s}} \simeq 330$ m/s). Therefore the incompressibility approximation (6) is well justified in atmospheric physics. In the ocean where the sound velocity is even larger and water velocities even smaller, this approximation is quite excellent.

Notice also that in realistic situations the temperature and density gradients in the entire turbulent boundary layer are sufficiently small such that the mean temperature and pressure difference on the mean-free path (which is about $6 \cdot 10^{-8}$ m in the air at atmospheric pressure and room temperature) are vanishingly small with respect to their mean values. This means that a local thermodynamic equilibrium exists with very hight accuracy and we can safety use a standard equation of state.

In the system (4) we have already neglected the viscous entropy production term assuming that the temperature gradients are large enough such that the thermal entropy production term dominates.

In quite air, without turbulence, the pressure and the density depend on the elevation z simply due to gravity. For example, in full thermodynamic equilibrium the temperature is uniform, z-independent, and the density decreases exponentially with the elevation. However, this equilibrium model of the atmosphere is not realistic, and cannot be used as a reference state about which the actual dynamics is considered. A much better reference state is a situation in which the entropy is space homogeneous. In this model the thermal conductivity (leading to the temperature homogeneity) is neglected with respect to heat transfer due to the vertical adiabatic mixing of air, leading to a z-independent entropy. Following tradition, we refer to the isentropic model as a "basic reference state" (BRS) and denote this state of the system with a subscript "$_{\mathrm{b}}$".

To proceed, we generalize the notion of potential temperature $\overline{\Theta}$ which is traditionally defined as the temperature that a volume of *dry air* at a pressure $p(z)$ and temperature $T(z)$ would attain when adiabatically compressed to a reference pressure, say, p_* that exists at zero elevation $z = 0$. This potential temperature can be explicitly computed for an ideal gas with the result

$$\overline{\Theta}(z) \equiv T(z)\,(p_*/p(z))^{1-c_{\mathrm{v}}/c_{\mathrm{p}}}\,, \tag{7}$$

there c_{V} and c_{P} are the air (fluid) specific heats at constant volume and pressure, respectively.

We want to generalize the notion of potential temperature for an arbitrary stratified fluid requiring that in the isenotropic basic reference state it would be a constant $\Theta_* = T_* \equiv T(0)$. A second requirement is that the definition will agree with Eq. 7 for an ideal gas. Accordingly we define

$$\overline{\Theta}(z) = T_* \exp\left[\left(\mathcal{S}(z) - \mathcal{S}_{\mathrm{b}}\right)/c_{\mathrm{p}}\right]. \tag{8}$$

For more details see also [16]. Indeed, if we employ the equation of state and the equation for the entropy of an ideal gas, i.e.

$$p = \rho T, \quad \mathcal{S} = \ln\left(p^{c_{\mathrm{v}}}/\rho^{c_{\mathrm{p}}}\right) + \mathrm{const}, \tag{9}$$

and remember, that $\mathcal{S}_{\mathrm{b}} = \mathcal{S}_* = \mathrm{const}$, one can easily check that Eq. 7 is recaptured.

For small deviations of $\overline{\Theta}$ from the basic reference state value T_*, Eq. 8 gives up to the linear order:

$$\Theta_{\mathrm{d}} \equiv \overline{\Theta} - T_* = T_* \hat{\mathcal{S}}\,/c_{\mathrm{p}}\,. \tag{10}$$

In the linear in Θ_d approximation the system (4) can be presented as [17]

$$\frac{\mathcal{D}\boldsymbol{\mathcal{U}}}{\mathcal{D}t} = -\boldsymbol{\nabla}\left(\frac{p}{\rho_b}\right) - \boldsymbol{\beta}\,\Theta_d + \frac{1}{\rho_b}(\boldsymbol{\nabla}\cdot\mu\boldsymbol{\nabla})\boldsymbol{\mathcal{U}}, \quad \frac{\mathcal{D}\,\Theta_d}{\mathcal{D}t} = \frac{1}{\rho_b}(\boldsymbol{\nabla}\cdot\kappa\boldsymbol{\nabla})\Theta_d. \tag{11}$$

Here $\mathcal{D}/\mathcal{D}t \equiv \partial/\partial t + \boldsymbol{\mathcal{U}}\cdot\boldsymbol{\nabla}$ is the convection time derivative, p—pressure, ρ_b is the density in BRS, $\boldsymbol{\beta} = \boldsymbol{g}\widetilde{\beta}$ is the buoyancy parameter ($\boldsymbol{\beta} = -\widehat{\boldsymbol{z}}\,\beta$, where $\widetilde{\beta} \equiv -(\partial\rho_b/\partial T_b)_p/\rho_b$ is the thermal expansion coefficient, which is equal to $1/T_b$ for an ideal gas), μ is the dynamic viscosity and κ is the dynamic thermal conductivity.

For simplicity of the following analysis we neglect in Eq. 11 terms, proportional to $d\rho_b(z)/dz$. Together with (6) this allows to simplify Eq. 11 up to the form:

$$\frac{\mathcal{D}\boldsymbol{\mathcal{U}}}{\mathcal{D}t} = -\frac{1}{\rho_b}\boldsymbol{\nabla}p - \boldsymbol{\beta}\,\Theta_d + \nu\Delta\boldsymbol{\mathcal{U}}, \quad \boldsymbol{\nabla}\boldsymbol{\mathcal{U}} = 0, \quad \frac{\mathcal{D}\,\Theta_d}{\mathcal{D}t} = \chi\,\Delta\Theta_d, \tag{12}$$

where ν—the kinematic viscosity and χ is the kinematic thermal conductivity.

Below, Eq. 12 will bring about an algebraic closure model with phenomenological parameters in Eq. 26 (c_{uu}, C_{SU}, etc.) independent of the elevation z. The vertical logarithmical derivative of ρ_b, i.e. $d\ln[\rho_b(z)]/dz$, is neglected in Eq. 12 with respect to (relative) gradients of the velocity and temperature fields on the outer scale of turbulence $\ell(z)$, which are accounted for in Eq. 11. An analysis of more general closure models which originate from Eq. 11 leads to relative corrections to the closure parameters of order $\ell(z)/H$, where $H \sim 10\,\mathrm{km}$ is the total height of the isentropic atmosphere. Under the assumption of saturation of $\ell(z) < L$, where $L \equiv \Lambda(0)$ is the Monin-Obukhov length defined below, the parameter ℓ/H is small for every elevation in the strongly stratified TBL with $L \ll H$. Without the assumption of ℓ-saturation, when $\ell(z)$ slowly increases with z for large elevations: $\ell(z) \simeq \widetilde{d}z$ with $\widetilde{d} = \mathrm{const} \ll 1$, then $\ell(z)/H \simeq \widetilde{d}z/H$ is still small because of the smallness of $\widetilde{d}$, even for z comparable with H. To conclude: the validity of the model with z-independent phenomenological parameters does not require the smallness of the elevation in the sense $z \ll H$, i.e. closeness of the air density $\rho_b(z)$ to its ground level $\rho_b(0)$.

We are not going to discuss here this issue in more details, but our strong feeling is that the ratio $\ell(z)/H \ll 1$ almost everywhere (especially in strongly stratified atmosphere) and thus z dependence of the closure parameters (that originate from the pressure drop with the elevation) can be peacefully neglected, at least in the main approximation.

It is important to realize that the *approximate* Eq. 12 *exactly* conserve an *approximate* expression for the total mechanic energy of the system in the dissipation-less limit. Consider the sum of the kinetic, $\mathcal{E}_K$, and the potential energy $\mathcal{E}_P$ (calculated in the basic reference state): $\mathcal{E}_t = \mathcal{E}_K + \mathcal{E}_P$,

$$\mathcal{E}_K \equiv \int dxdydz\,\rho_b\,\frac{|\boldsymbol{\mathcal{U}}|^2}{2}, \quad \mathcal{E}_P \equiv \int dxdydz\,\rho_b\beta z\Theta_d. \tag{13}$$

One can check by direct substitution that this sum of energies is conserved by Eq. 12 when $\nu = \chi = 0$.

To develop equations for mean quantities and correlation functions one applies the Reynolds decomposition $\boldsymbol{\mathcal{U}} = \boldsymbol{U} + \boldsymbol{u}$, $\langle\boldsymbol{\mathcal{U}}\rangle = \boldsymbol{U}$, $\langle\boldsymbol{u}\rangle = 0$, $\Theta_d = \Theta + \theta$, $\langle\Theta_d\rangle = \Theta$, $\langle\theta\rangle = 0$, $p = \langle p\rangle + \widetilde{p}$, $\langle\widetilde{p}\rangle = 0$. Here $\langle\cdots\rangle$ stands for a "proper" averaging, e.g. in plain geometry this can be an averaging over a horizontal plane at a constant elevation when the average quantities depend on $(z,\,t)$ only. Substituting in Eq. 12 one gets equations of motion for the mean velocity and mean temperature profiles

$$\frac{D\,U_i}{Dt} + \nabla_j\,\widetilde{\tau}_{ij} = -\frac{\nabla_i\langle p\rangle}{\rho_b} - \beta_i\Theta, \quad \frac{D\,\Theta}{Dt} + \boldsymbol{\nabla}\cdot\widetilde{\boldsymbol{F}} = 0. \tag{14}$$

Here $D/Dt \equiv \partial/\partial t + \boldsymbol{U}\cdot\boldsymbol{\nabla}$ is the mean convection derivative. The total (molecular and turbulent) momentum and thermal fluxes are

$$\widetilde{\tau}_{ij} \equiv -\nu\nabla_j U_i + \tau_{ij}, \quad \widetilde{\boldsymbol{F}} \equiv -\chi\,\boldsymbol{\nabla}\Theta + \boldsymbol{F}, \tag{15}$$

where $\tau_{ij} = \langle u_i u_j\rangle$ is the Reynolds stress tensor describing the turbulent momentum flux, and $\boldsymbol{F} = \langle \boldsymbol{u}\theta\rangle$ is the turbulent thermal flux. In order to derive equations for these correlation functions, one considers the equations of motion for the fluctuating velocity and temperature:

$$D\,\boldsymbol{u}/D\,t = -\boldsymbol{u}\cdot\boldsymbol{\nabla}\boldsymbol{U} - \boldsymbol{u}\cdot\boldsymbol{\nabla}\boldsymbol{u} + \langle \boldsymbol{u}\cdot\boldsymbol{\nabla}\boldsymbol{u}\rangle - (\boldsymbol{\nabla}\widetilde{p}/\rho_b) + \nu\,\Delta\boldsymbol{u} - \boldsymbol{\beta}\,\theta, \tag{16a}$$

$$D\,\theta/D\,t = -\boldsymbol{u}\cdot\boldsymbol{\nabla}\Theta - \boldsymbol{u}\cdot\boldsymbol{\nabla}\theta + \chi\,\Delta\theta + \langle \boldsymbol{u}\cdot\boldsymbol{\nabla}\theta\rangle\,. \tag{16b}$$

The whole set of the second order correlation functions includes the Reynolds stress, τ_{ij}, the turbulent thermal flux, $\boldsymbol{F}$, and the "temperature energy" $E_\theta \equiv \langle\theta^2\rangle/2$, which is denoted and named by analogy with the turbulent kinetic energy density (per unit mass and unit volume), $E_\mathrm{K} = \langle|\boldsymbol{u}|^2\rangle/2 = \mathrm{Tr}\{\tau_{ij}\}/2$. Notice, that an importance of E_θ was recognized and explored already in [3,18–25]. Using (16) one gets the following "balance equations":

$$\frac{D\,\tau_{ij}}{Dt} + \varepsilon_{ij} + \frac{\partial}{\partial x_k}\mathcal{W}_{ijk} = \mathcal{P}_{ij} - \mathcal{C}_{ij} + \mathcal{R}_{ij}, \tag{17a}$$

$$\frac{D\,F_i}{Dt} + \varepsilon_i + \frac{\partial}{\partial x_j}\mathcal{W}_{ij} = \mathcal{A}_i + \mathcal{B}_i, \tag{17b}$$

$$\frac{D\,E_\theta}{D\,t} + \varepsilon + \boldsymbol{\nabla}\cdot\boldsymbol{\mathcal{W}} = -\boldsymbol{F}\cdot\boldsymbol{\nabla}\Theta. \tag{17c}$$

Here we denoted the dissipations of the Reynolds-stress, heat-flux and the temperature energy by

$$\varepsilon_{ij} \equiv 2\,\nu\left\langle\frac{\partial u_i}{\partial x_k}\,\frac{\partial u_j}{\partial x_k}\right\rangle, \quad \varepsilon_i \equiv (\nu+\chi)\left\langle\frac{\partial\theta}{\partial x_k}\,\frac{\partial u_i}{\partial x_k}\right\rangle, \quad \varepsilon \equiv \chi\,\left\langle|\boldsymbol{\nabla}\theta|^2\right\rangle. \tag{18}$$

The last term on the LHS of each of Eq. 17 describes a *spatial* flux of the corresponding quantity. In models of wall bounded unstratified turbulence it is known that these terms are very small almost everywhere, see e.g. [26]. We do not have sufficient experience with the stratified counterpart to be able to assert that the same is true here. Nevertheless, for simplicity we are going to follow the traditional assumption [10] and to neglect these terms. It is possible to show that the accounting for these terms does not influence much the results. Note that keeping these terms turns the model into a set of differential equations which are very cumbersome to analyze.

The first term on the RHS of the balance Eq. 17a for the Reynolds stresses is the "Energy Production tensor" $\mathcal{P}_{ij}$, describing the production of the turbulent kinetic energy from the kinetic energy of the mean flow, proportional to the gradient of the mean velocity:

$$\mathcal{P}_{ij} \equiv -\tau_{ik}\,\partial U_j/\partial x_k - \tau_{jk}\,\partial U_i/\partial x_k. \tag{19a}$$

The second term on the RHS of Eq. 17a, $\mathcal{C}_{ij}$, will be referred hereafter to as the "Energy Conversion tensor". It describes the conversion of the turbulent kinetic energy into turbulent potential energy. This term is proportional to the buoyancy parameter β and the turbulent thermal flux $\boldsymbol{F}$:

$$\mathcal{C}_{ij} \equiv -\beta\left(F_i\,\delta_{j\,z} + F_j\,\delta_{i\,z}\right), \tag{19b}$$

where δ_{iz} is Kronecker delta. The last term in the RHS of Eq. 17a is known as the "Pressure-rate-of-strain tensor":

$$\mathcal{R}_{ij} \equiv \left\langle \widetilde{p}\, s_{ij}/\rho_{\rm b} \right\rangle, \quad s_{ij} \equiv \partial u_i/\partial x_j + \partial u_j/\partial x_i. \tag{19c}$$

In incompressible turbulence its trace vanishes, therefore $\mathcal{R}_{ij}$ does not contribute to the balance of the kinetic energy. As we will show in Sect. 3.1, this tensor can be presented as the sum of three contributions [3],

$$\mathcal{R}_{ij} = R^{\rm RI}_{ij} + R^{\rm IP}_{ij} + R^{\rm IC}_{ij}, \tag{19d}$$

in which $R^{\rm RI}_{ij}$ is responsible for the nonlinear process of isotropization of turbulence and is traditionally called the "Return-to-Isotropy", $R^{\rm IP}_{ij}$ is similar to the energy production tensor (19a) and is called "Isotropization of Production". A new term, appearing in the stratified flow, $R^{\rm IC}_{ij}$, is similar to the energy conversion tensor (19b) and will be refereed to as the "Isotropization of Conversion".

Consider the balance of the turbulent thermal flux $\boldsymbol{F}$, Eq. 17b. The first term in the RHS, $\boldsymbol{\mathcal{A}}$, describes the source of $\boldsymbol{F}$ and, by analogy with the energy-production tensor, $\mathcal{P}_{ij}$, is called "Thermal-flux production vector". Like $\mathcal{P}_{ij}$ it has the contribution, A_i^{SU}, proportional to the mean velocity gradient:

$$\begin{aligned} \mathcal{A}_i &\equiv A_i^{SU} + A_i^{S\Theta} + A_i^{E\theta}, \quad A_i^{SU} \equiv -\boldsymbol{F}\cdot\boldsymbol{\nabla}\, U_i, \\ A_i^{S\Theta} &\equiv -\tau_{ij}\,\partial\Theta/\partial x_j, \quad A_i^{E\theta} \equiv 2\,\beta\, E_\theta\, \delta_{i\,z}, \end{aligned} \tag{19e}$$

and two additional contributions, related to the temperature gradient and to the "temperature energy", E_θ, and the buoyancy parameter. One sees, that in contrary to the oversimplified assumption (2b), the thermal flux in such a turbulent media cannot be considered as proportional to the temperature gradient. It has also a contribution proportional to the velocity gradient and even to the square of the temperature fluctuations. Moreover, the RHS of the flux-balance Eq. 17b has an additional term, the "Pressure-temperature-gradient vector" which, similarly to the pressure-rate-of-strain tensor (19d), can be divided into three parts [3]:

$$\boldsymbol{\mathcal{B}} \equiv \langle \widetilde{p}\,\boldsymbol{\nabla}\theta/\rho_b\rangle = \boldsymbol{B}^{\rm RD} + \boldsymbol{B}^{\rm SU} + \boldsymbol{B}^{{\rm E}\theta}. \tag{19f}$$

As we will show in Sect. 3.1 the first contribution, $B_i^{\rm RD} \propto \langle u\, u\, \nabla_i\, \theta\rangle$ is responsible for the nonlinear flux of $\boldsymbol{F}$ in the space of scales toward smaller scales, similarly to the correlation $\langle u\, u\, u\rangle$, which is responsible for the flux of kinetic energy $\langle u2\rangle/2$ toward smaller scales. The correlation $B_i^{\rm RD} \propto \langle u\, u\, \nabla_i\, \theta\rangle$ may be understood as the nonlinear contribution to the dissipation of the thermal flux. Correspondingly we will call it "Renormalization of the thermal-flux Dissipation" and will supply it with a superscript "RD". The next two terms in the decomposition (19f) are $B_i^{SU} \propto S_{\rm U}$ and $B_i^{E\theta} \propto E_\theta$. They describe the renormalization of the thermal-flux production terms $A_i^{SU} \propto S_{\rm U}$ and $A_i^{E\theta} \propto E_\theta$, accordingly.

2.2 Conservation of total mechanical energy in the exact balance equations

The total mechanical energy of temperature stratified turbulent flows consists of three parts with densities (per unit mass): $E = E_{\mathcal{K}} + E_{\rm K} + E_{\rm P}$, where $E_{\mathcal{K}} = |\boldsymbol{U}|^2/2$ is the density of kinetic energy of the mean flow, $E_{\rm K} = \tau_{ii}/2$ is the density of turbulent kinetic energy and $E_{\rm P} = \beta E_\theta/S_\Theta$ is the density of potential energy, associated with turbulent density fluctuation $\widetilde{\rho} = \widetilde{\beta}\,\theta\rho_b$, caused by the (potential) temperature fluctuations θ, and $S_\Theta = d\,\Theta/dz$. Note that the formula for $E_{\rm P}$ appears different from $\mathcal{E}_{\rm P}$ in Eq. 13. It is possible to show that in

fact the difference between the two objects is a time independent total potential energy in the basics reference state, and therefore it can be considered as the zero level of the potential energy.

The balance equation for $E_{\mathcal{K}}$ follows from Eq. 14:

$$DE_{\mathcal{K}}/Dt + \nu \left(\nabla_j U_i\right) 2 + \nabla_j \left(U_i \widetilde{\tau}_{ij}\right) = [\text{source} E_{\mathcal{K}}] + \tau_{ij} \nabla_j U_i, \tag{20a}$$

with the help of identity: $U_i \nabla_j \tau_{ij} \equiv \nabla_j \left(U_i \tau_{ij}\right) - \tau_{ij} \nabla_j U_i$ and definition (15). The terms on the LHS of this equation, proportional to ν and $\widetilde{\tau}_{ij}$ respectively, describe the dissipation and the spatial flux of $E_{\mathcal{K}}$. The term [source $E_{\mathcal{K}}$] on the RHS of Eq. 20a describes the external source of energy, originating from the boundary conditions described above, and $\tau_{ij} \nabla_j U_i$ describes the kinetic energy out-flux from the mean flow to turbulent subsystem.

The balance equation for the turbulent kinetic energy follows directly from Eq. 17a:

$$DE_{\mathrm{K}}/Dt + \left[\varepsilon_{ii} + \nabla_j \mathcal{W}_{iij}\right]/2 = -\tau_{ij} \nabla_j U_i + \beta F_z. \tag{20b}$$

On the LHS of Eq. 20b one sees the dissipation and spatial flux terms. The first term on the RHS originates from the energy production, $\frac{1}{2} \mathcal{P}_{ii}$, defined by Eq. 19a. This term has an opposite sign to the last term on the RHS of Eq. 20a and describes the production of the turbulent kinetic energy from the kinetic energy of the mean flow. The last term on the RHS of Eq. 20b originates from the energy conversion tensor $\frac{1}{2} \mathcal{C}_{ii}$, Eq. 19b, and describes the conversion of the turbulent kinetic energy into potential one.

According to the last of Eq. 17, one gets the balance equation for the potential energy E_{P}; multiplying Eq. 17c for E_θ by β/S_Θ:

$$DE_{\mathrm{P}}/Dt + \beta \left[\varepsilon + \nabla_j \mathcal{W}_j\right]/S_\Theta = -\beta F_z. \tag{20c}$$

The RHS of this equation [coinciding up to a sign with the last term on the RHS of Eq. 20b] is the source of potential energy (from the kinetic one).

Summing up the above three equations, one gets the total mechanical energy balance:

$$DE/Dt + [\text{diss} E] + \boldsymbol{\nabla} [\text{flux} E] = [\text{source} E_{\mathcal{K}}]. \tag{21}$$

This equation exactly respects the conservation of total mechanical energy in the dissipationless limit, irrespective of the closure approximations. This is because the energy production and conversion terms are exact and do not require any closures, while the pressure-rate-of-strain tensor, that requires some closure, does not contribute to the total energy balance.

3 The closure procedure and the resulting model

In this section we describe the proposed closure procedure that results in a model of stably stratified TBL. In developing this model we strongly rely on the analogous well developed modeling of standard (unstratified) TBL. The final justification of this approach can be done only in comparison to data from experiments and simulations. We will do below what we can to use the existing data, but we propose at this point that much more experimental and simulational work is necessary to solidify all the steps taken in this section.

3.1 Pressure-rate-of-strain tensor $\mathcal{R}_{ij}$ and Pressure-temperature-gradient vector $\mathcal{B}$

The correlation functions $\mathcal{R}_{ij}$ and $\boldsymbol{\mathcal{B}}$, defined by Eqs. 19c and 19f, include fluctuating part of the pressure $\widetilde{p}$. The Poisson's equation for $\widetilde{p}$ follows from Eq. 16:

$\Delta\widetilde{p} = \rho_{\rm b}\left[-\nabla_i\nabla_j\left(u_iu_j - \langle u_iu_j\rangle + U_iu_j + U_ju_i\right) + \beta\nabla_z\theta\right]$. The solution of this equation includes a harmonic part, $\Delta\widetilde{p} = 0$, which is responsible for sound propagation and does not contribute to turbulent dynamics at small Mach numbers. Thus this contribution can be neglected. The inhomogeneous solution includes three parts $\widetilde{p} = \rho_{\rm b}[p_{uu} + p_{Uu} + p_\theta]$, where

$$p_{uu} = \Delta^{-1}\nabla_i\nabla_j\left(\langle u_iu_j\rangle - u_iu_j\right), \tag{22}$$

$$p_{Uu} = \Delta^{-1}\nabla_i\nabla_j\left(U_iu_j + U_ju_i\right), \tag{23}$$

$$p_\theta = \beta\Delta^{-1}\nabla_z\,\theta, \tag{24}$$

and the inverse Laplace operator Δ^{-1} is defined as usual in terms of an integral over the Green's function.

Correspondingly the correlations $\mathcal{R}_{ij}$ and $\boldsymbol{\mathcal{B}}$ consist of three terms, Eqs. 19d and 19f, in which

$$\begin{aligned} &R_{ij}^{\rm RI} = \langle p_{uu}s_{ij}\rangle, \quad R_{ij}^{\rm IP} \equiv \langle p_{Uu}\,s_{ij}\rangle, \quad R_{ij}^{\rm IC} \equiv \langle p_\theta s_{ij}\rangle, \\ &\boldsymbol{B}_i^{\rm RD} = \langle p_{uu}\nabla\theta\rangle, \quad \boldsymbol{B}^{SU} \equiv \langle p_{Uu}\nabla\theta\rangle, \quad \boldsymbol{B}_i^{E\theta} \equiv \langle p_\theta\nabla\theta\rangle. \end{aligned} \tag{25}$$

All of those terms originating from p_{uu} are the most problematic because they introduce coupling to triple correlation functions: $R_{ij}^{\rm RI} \propto \langle u_iu_ju_k\rangle$ and $\boldsymbol{B}^{\rm RD} \propto \langle u^2\nabla\theta\rangle$. Thus they require closure procedures whose justification can be only tested a-posteriori against the data.

Having in mind to simplify the model in most possible manner, we adopt for the diagonal part of the Return-to-Isotropy tensor, the simplest Rota form [27]

$$R_{ii}^{\rm RI} \simeq -\gamma_{\rm RI}\left(\tau_{ii} - 2\,E_{\rm K}/3\right), \tag{26a}$$

in which $\gamma_{\rm RI}$ can be understood as a relaxation frequency (or inverse relaxation time) of diagonal components of the Reynolds-stress tensor toward its isotropic form, $2E_{\rm K}/3$. The parametrization of $\gamma_{\rm RI}$ will be discussed later. The tensor $R_{ij}^{\rm RI}$ is traceless, therefore the frequency $\gamma_{\rm RI}$ must be the same for all the diagonal components of $R_{ii}^{\rm RI}$. On the other hand there are no reasons to assume that off-diagonal terms have the same relaxation frequency. Therefore, following [28] we assume that

$$R_{ij}^{\rm RI} \simeq -\widetilde{\gamma}_{\rm RI}\tau_{ij}, \quad i \neq j, \tag{26b}$$

with, generally speaking, $\widetilde{\gamma}_{\rm RI} \neq \gamma_{\rm RI}$. Moreover, on the intuitive level we can expect that off-diagonal terms should decay faster then the diagonal ones, i.e. $\widetilde{\gamma}_{\rm RI} > \gamma_{\rm RI}$. Indeed, our analysis of DNS results shows that $\widetilde{\gamma}_{\rm RI}/\gamma_{\rm RI} \simeq 1.46$ [29].

The term $\boldsymbol{B}^{\rm RD}$ also describes return-to-isotropy due to nonlinear turbulence self interactions [3], and may be modeled as:

$$B_i^{\rm RD} = -\gamma_{\rm RD}F_i. \tag{26c}$$

This equation dictates the vectorial structure of $B_i^{\rm RD} \propto F_i$, which will be confirmed below. The rest can be understood as the definition of the $\gamma_{\rm RD}$ as the relaxation frequency of the thermal flux. Its parametrization is the subject of further discussion in Sect. 3.4.

The traceless "Isotropization-of-Production" tensor, $R_{ij}^{\rm IP}$, has a very similar structure to the production tensor, $\mathcal{P}_{ij}$, Eq. 19a, and thus is traditionally modeled in terms of $\mathcal{P}_{ij}$ [26]:

$$R_{ij}^{\rm IP} \simeq -C_{\rm IP}\left(P_{ij} - \delta_{ij}\,\mathcal{P}/3\right), \quad \mathcal{P} \equiv {\rm Tr}\,\{P_{ij}\}. \tag{26d}$$

The accepted value of the numerical constant $C_{\rm IP} = \frac{3}{5}$ [26].

The traceless "Isotropization-of-Conversion" tensor, $R^{\rm IC}_{ij}$ does not exist in unstratified TBL. Its structure is very similar to the conversion tensor, $\mathcal{C}_{ij}$, Eq. 19b. Therefore it is reasonable to model it in the same way in terms of $\mathcal{C}_{ij}$ [3]:

$$R^{\rm IC}_{ij} \simeq -C_{\rm IC}\left(\mathcal{C}_{ij} - \delta_{ij}\,\mathcal{C}/3\right), \quad \mathcal{C} \equiv {\rm Tr}\,\{\mathcal{C}_{ij}\}, \tag{26e}$$

with some new constant $C_{\rm IC}$.

The renormalization of production terms B_i^{SU} and $B_i^{E\theta}$ are very similar to the corresponding thermal flux production terms, A_i^{SU} and $A_i^{E\theta}$, defined by Eq. 19e. Therefore, in the spirit of Eqs. 26d and 26e, they are modeled as follows:

$$B_i^{SU} = (C_{SU} - 1)A_i^{SU} = (1 - C_{SU})(\boldsymbol{F}\cdot\boldsymbol{\nabla})U_i, \tag{26f}$$

$$B_i^{E\theta} = -(C_{E\theta} + 1)A_i^{E\theta} = -2\,\beta\,(C_{E\theta} + 1)E_\theta\,\delta_{i\,z}. \tag{26g}$$

Using this and (24) one finds the sign of $C_{E\theta}$:

$$-\beta\left(C_{E\theta} + 1\right)E_\theta = \langle p_\theta \nabla_z \theta\rangle = \beta\langle(\nabla_z\theta)\Delta^{-1}(\nabla_z\theta)\rangle,$$
$$C_{E\theta} = -\left(1 + \langle(\nabla_z\theta)\Delta^{-1}(\nabla_z\theta)\rangle/\langle\theta^2\rangle\right) < 0. \tag{27}$$

To estimate $C_{E\theta}$ we assume that on the gradient scales the temperature fluctuations are roughly isotropic [9], and therefore we can estimate $\Delta = \nabla_x^2 + \nabla_y^2 + \nabla_z^2 \approx 3\nabla_z^2$. Introducing this estimate and integrating by parts leads to $C_{E\theta} \approx -2/3$.

3.2 Reynolds-stress-, thermal-flux-, and thermal-dissipation

Far away from the wall and for large Reynolds numbers the dissipation tensors are dominated by the viscous scale motions, at which turbulence can be considered as isotropic. Therefore, the vector $\boldsymbol{\varepsilon}$ should vanish, while the tensor ε_{ij} should be diagonal:

$$\varepsilon_i = 0, \quad \varepsilon_{ij} = 2\,\gamma_{uu}\,E_{\rm K}\,\delta_{ij}/3, \tag{28a}$$

where the numerical prefactor $\frac{2}{3}$ is chosen such that γ_{uu} becomes the relaxation frequency of the turbulent kinetic energy. Under stationary conditions the rate of turbulent kinetic energy dissipation is equal to the energy flux through scales, that can be estimated as $\langle uuu\rangle/\ell$, where ℓ is the outer scale of turbulence. Therefore, the natural estimate of γ_{uu} involves the triple-velocity correlator, $\gamma_{uu} \sim (\langle uuu\rangle/\ell\,\langle uu\rangle)$, exactly in the same manner, as the Return-to-Isotropy frequencies, $\gamma_{\rm RI}$ and $\widetilde{\gamma}_{\rm RI}$ in Eqs. 26a and 26b. Similarly,

$$\varepsilon = \gamma_{\theta\theta}\,E_\theta, \quad \gamma_{\theta\theta} \sim \langle\theta\theta u\rangle\,\big/\,\ell\,\langle\theta\theta\rangle\,. \tag{28b}$$

3.3 Stationary balance equations in plain geometry

In the plane geometry, the equations simplify further. The mean velocity is oriented in the (streamwise) $\widehat{\mathbf{x}}$ direction and all mean values depend on the vertical (wall-normal) coordinate z only: $\boldsymbol{U} = U(z)\,\widehat{\mathbf{x}}$, $\Theta = \Theta(z)$, $\tau_{ij} = \tau_{ij}(z)$, $\boldsymbol{F} = \boldsymbol{F}(z)$, $E_\theta = E_\theta(z)$. Therefore $(\boldsymbol{U}\cdot\boldsymbol{\nabla})\,\langle\cdots\rangle = 0$, and in the stationary case, when $\partial/\partial t = 0$, the mean convective derivative vanishes: $D/D\,t = 0$. Moreover due to the $y \to -y$ symmetry of the problem the following correlations vanish: $\widetilde{\tau}_{xy} = \widetilde{\tau}_{yz} = \widetilde{F}_y = 0$. The only non-zero components of the mean velocity and temperature gradients are:

$$S_U \equiv dU/dz, \quad S_\Theta \equiv d\Theta/dz. \tag{29}$$

3.3.1 Equations for the mean velocity and temperature profiles

Having in mind equations of Sect. 3.3 and integrating Eq. 14 for U_x and Θ over z, one gets equations for the total (turbulent and molecular) mechanical-momentum flux, $\widetilde{\tau}(z)$, and thermal flux, $\widetilde{F}(z)$, toward the wall

$$\widetilde{\tau}_{xz}(z) = -\nu\, S_U + \tau_{xz} \tag{30a}$$

$$\widetilde{F}_z(z) = -\chi\, S_\Theta + F_z \tag{30b}$$

The total flux of the x-component of the mechanical moment in z-direction is $\widetilde{\tau}_{xz}(z) \equiv \int dz(\partial \langle p\rangle / \partial x) + \text{const}$. Generally speaking, $\widetilde{\tau}_{xz}(z)$ depends on z. For example, for the unstratified pressure driven planar channel flow (of the half-wight h) $\widetilde{\tau}_{xz}(z) = -\tau_*(1-x/h)$, where τ_* is the wall shear stress. In the stable atmospheric TBL Nieuwstadt [10] suggested the momentum and temperature flux profiles in the form:

$$\widetilde{\tau}_{xz}(z) = -\tau_*\, f_1(z), \quad f_1(z) = [1 - z/H_Z]^{3/2}, \tag{31a}$$

$$\widetilde{F}_z(z) = -F_*\, f_2(z), \quad f_2(z) = 1 - z/H_Z, \tag{31b}$$

where F_* is the heat flux at the ground and H_Z is the Zilitinkevich height of stratified TBL [15]. Notice, that in our case of stable stratification both vertical fluxes, the x-component of the mechanical momentum, $\widetilde{\tau}_{xz}$, and the thermal flux, $\widetilde{F}_z$, are directed toward the ground, i.e. negative. For the sake of convenience, we introduce in Eq. 31 notations for their (positive) zero level absolute value: τ_* and F_*. In the future analysis we will consider the flux profiles $f_1(z)$ and $f_2(z)$ as prescribed functions of z, not necessarily given by Eq. 31.

Recall that in the plain geometry $U_z = 0$. Nevertheless one can write an equation for U_z:

$$d\left(\tau_{zz} + \langle p\rangle / \rho_b\right)/dz = \beta\,\Theta, \tag{32}$$

which describes a turbulent correction to the hydrostatic equilibrium. Actually, this equation determines the profile of $\langle p\rangle$, that does not appear in the system of balance Eq. 30.

3.3.2 Equations for the pair (cross)-correlation functions

Consider first the balance Eq. 17a for the diagonal components of the Reynolds-stress tensor in the plain geometry:

$$\begin{aligned}
\Gamma E_\mathrm{K} + 3\gamma_\mathrm{RI}\tau_{xx}/2 &= -\left(3 - 2\,C_\mathrm{IP}\right)\tau_{xz}S_U - C_\mathrm{IC}\,\beta\,F_z,\\
\Gamma E_\mathrm{K} + 3\gamma_\mathrm{RI}\tau_{yy}/2 &= -C_\mathrm{IP}\tau_{xz}S_U - C_\mathrm{IC}\,\beta\,F_z,\\
\Gamma E_\mathrm{K} + 3\gamma_\mathrm{RI}\tau_{zz}/2 &= -C_\mathrm{IP}\tau_{xz}S_U + \left(3 + 2\,C_\mathrm{IC}\right)\beta\,F_z.
\end{aligned} \tag{33}$$

where $\Gamma \equiv \gamma_{uu} - \gamma_\mathrm{RI}$. The LHS of these equations includes the dissipation and Return-to-isotropy terms. On the RHS we have the kinetic energy production and isotropization of production terms (both proportional to S_U) together with the conversion and isotropization of conversion terms, that are proportional to the vertical thermal flux F_z.

System (33) allows to find anisotropy of the turbulent-velocity fluctuations and to get the balance equations for the turbulent kinetic energy with the energy production and conversion terms on the RHS:

$$3\tau_{xx} = 2\left\{[2(1 - C_\mathrm{IP})\Gamma_{uu}/\gamma_\mathrm{RI} + 1]E_\mathrm{K} - (3 - 2C_\mathrm{IP} + C_\mathrm{IC})\,\beta F_z/\gamma_\mathrm{RI}\right\}, \tag{34a}$$

$$3\tau_{yy} = 2\left\{[(C_\mathrm{IP} - 1)\Gamma_{uu}/\gamma_\mathrm{RI} + 1]E_\mathrm{K} - (C_\mathrm{IP} + C_\mathrm{IC})\beta F_z/\gamma_\mathrm{RI}\right\}, \tag{34b}$$

$$3\tau_{zz} = 2\left\{[(C_\mathrm{IP} - 1)\,\Gamma_{uu}/\gamma_\mathrm{RI} + 1]E_\mathrm{K} - (C_\mathrm{IP} - 2C_\mathrm{IC} - 3)\,\beta F_z/\gamma_\mathrm{RI}\right\}, \tag{34c}$$

$$\Gamma_{uu} E_{\mathrm{K}} = -\tau_{xz} S_U + \beta F_z. \tag{34d}$$

Equation 34d includes the only non-vanishing tangential (off-diagonal) Reynolds stress τ_{xz} and has to be accompanied with an equation for this object:

$$\widetilde{\gamma}_{\mathrm{RI}} \tau_{xz} = (C_{\mathrm{IP}} - 1)\, \tau_{zz}\, S_U + (1 + C_{\mathrm{IC}})\, \beta\, F_x. \tag{34e}$$

This equation manifests that the tangential Reynolds stress τ_{xz}, that determines the energy production influences, in its turn, on the value of the streamwise thermal flux F_x, which therefore effects on the turbulent kinetic energy production.

As we mentioned, in the plain geometry $\widetilde{F}_y = 0$. Equation (17b) for the F_x and F_z in this case take the form:

$$\gamma_{\mathrm{RD}} F_x = -\left(\tau_{xz} S_\Theta + C_{\mathrm{SU}} F_z S_U\right), \tag{35a}$$
$$\gamma_{\mathrm{RD}} F_z = -\left(\tau_{zz} S_\Theta + 2\, C_{\mathrm{E}\Theta}\, \beta E_\theta\right), \tag{35b}$$

in which the RHS describes the thermal-flux production, corrected by the isotropization of production terms.

The last Eq. 17c for E_θ, represents the balance between the dissipation (LHS) and production (RHS):

$$\gamma_{\theta\theta}\, E_\theta = -F_z\, S_\Theta. \tag{35c}$$

3.4 Dimensional closure of time-scales and the balance equations in the turbulent region

At this point we follow the tradition in modeling of all the nonlinear inverse time-scales by dimensional estimates [30]:

$$\begin{aligned} &\gamma_{uu} = c_{uu} \sqrt{E_{\mathrm{K}}}\, / \ell\,, \\ &\gamma_{\mathrm{RI}} = C_{\mathrm{RI}} \gamma_{uu}, \quad \widetilde{\gamma}_{\mathrm{RI}} = \widetilde{C}_{\mathrm{RI}} \gamma_{\mathrm{RI}}, \quad \gamma_{\theta\theta} = C_{\theta\theta} \gamma_{uu}, \quad \gamma_{\mathrm{RD}} = C_{u\theta} \gamma_{uu}. \end{aligned} \tag{36}$$

Here ℓ is still the "outer scale of turbulence".

Detailed analysis of experimental, DNS and LES data (see [28] and references therein) shows that for unstratified flows, $\mathrm{g} = 0$, the anisotropic boundary layers exhibit values of the Reynolds stress tensor that can be well approximated by $\tau_{xx} = E_{\mathrm{K}}$, $\tau_{yy} = \tau_{zz} = E_{\mathrm{K}}/2$. In our approach this dictates the choice $C_{\mathrm{RI}} = 4(1 - C_{\mathrm{IP}})$. Also we can expect that τ_{yy} is almost not affected by buoyancy. This gives simply $C_{\mathrm{IC}} = -C_{\mathrm{IP}}$. If so, Eq. 34 with the parametrization (36) can be identically rewritten as follows:

$$\begin{aligned} &\tau_{xx} = E_{\mathrm{K}} - \frac{\beta F_z}{2\,\gamma_{uu}}, \quad \tau_{yy} = \frac{E_{\mathrm{K}}}{2}, \quad \tau_{zz} = \frac{E_{\mathrm{K}}}{2} + \frac{\beta F_z}{2\,\gamma_{uu}}, \\ &\gamma_{uu} E_{\mathrm{K}} = \beta F_z - \tau_{xz} S_U, \quad 4\,\widetilde{C}_{\mathrm{RI}}\, \gamma_{uu} \tau_{xz} = \beta\, F_x - \tau_{zz}\, S_U. \end{aligned} \tag{37a}$$

Finally we present a version of the balance equations for the thermal flux (35a, 35b), and for the "temperature energy", (35c), after all the simplified assumptions:

$$\begin{aligned} C_{\theta\theta}\, \gamma_{uu} E_\theta &= -F_z\, S_\Theta, \\ C_{u\theta}\, \gamma_{uu} F_x &= -\left(\tau_{xz} S_\Theta + C_{\mathrm{SU}} F_z\, S_U\right), \\ C_{u\theta}\, \gamma_{uu} F_z &= -\left(\tau_{zz} S_\Theta + 2\, C_{\mathrm{E}\Theta}\, \beta E_\theta\right). \end{aligned} \tag{37b}$$

3.5 Generalized wall normalization

The analysis of the balance Eq. 37 is drastically simplified if they are presented in a dimensionless form. Traditionally, the conventional "wall units" are introduced via the wall friction velocity, $u_* \equiv \sqrt{\tau_*}$, and the viscous length-scale, λ_*, defined by $\lambda_* \equiv \nu/u_*$. A wall unit for the temperature, $\theta_* \equiv F_*/u_*$, is defined via the thermal flux at the wall and friction velocity. Subsequently, $\boldsymbol{r}^+ \equiv \boldsymbol{r}/\lambda_*$, $t^+ \equiv t\,\lambda_*/u_*$, $\boldsymbol{\mathcal{U}}^+ \equiv \boldsymbol{\mathcal{U}}/u_*$, $p^+ \equiv p/\rho_b\, u_*^2$, $\Theta^+ \equiv \Theta/\theta_*$, $\theta^+ \equiv \theta/\theta_*$, etc. Then the governing Eq. 12 take the form:

$$\begin{aligned} \mathcal{D}^+\boldsymbol{\mathcal{U}}^+/\mathcal{D}t^+ + \boldsymbol{\nabla}^+ p^+ &= \widehat{\boldsymbol{z}}\,\Theta_{\mathrm{d}}^+/L^+ + \Delta^+\boldsymbol{\mathcal{U}}^+, \\ \mathcal{D}^+\,\Theta_{\mathrm{d}}^+/\mathcal{D}t^+ &= \Delta^+\,\Theta_{\mathrm{d}}^+/\mathrm{Pr}. \end{aligned} \tag{38}$$

These equations include two dimensionless parameters: the conventional Prandtl number $\mathrm{Pr} = \nu/\kappa$, and L^+—the Monin-Obukhov length L measured in wall units: $L \equiv u_*^3/\beta F_*$, $L^+ \equiv L/\lambda_*$. We used here the modern definition of the Monin-Obukhov length, which differs from the old one by the absence of the von-Kármánconstant κ in its denominator [31].

Outside of the viscous sub-layer, where the kinematic viscosity and kinematic thermal conductivity can be ignored, L^+ is the only dimensionless parameter in the problem, which separates the region of weak stratification, $z^+ < L^+$, and the region of strong stratification, where $z^+ > L^+$.

Given the generalized wall normalization we introduce objects with a superscript "$^+$" in the usual manner:

$$\begin{aligned} &S_U^+ \equiv t_*\,S_U,\; S_\Theta^+ \equiv \lambda_*\,S_\Theta/\theta_*,\; \gamma^+ \equiv t_*\gamma,\; \tau_{ij}^+ \equiv \tau_{ij}/u_*^2, \\ &\boldsymbol{F}^+ \equiv \boldsymbol{F}/u_*\theta_*,\; E_\theta^+ \equiv E_\theta/\theta_*^2. \end{aligned} \tag{39}$$

In the turbulent region, governed by L^+ only, Eq. 30 simplify to $\tau_{xz}^+ = -f_1$, $F_z^+ = -f_2$.

3.6 Rescaling symmetry and ‡-representation

Outside of the viscous region, where Eq. 37 were derived, the problem has only one characteristic length, i.e. the Monin-Obukhov scale L, defined via fluxes on the ground. With fluxes depending on the elevation in the local closure equations the scale L is replaced by local Monin-Obukhov length $\Lambda(z)$ [10], defined similarly via local fluxes:

$$\Lambda(z) \equiv -\frac{|\tau_{xz}(z)|^{3/2}}{\beta F_z(z)} = -L\,\frac{|\tau_{xz}^+(z)|^{3/2}}{F_z^+(z)} = L\frac{{f_1}^{3/2}(z)}{f_2(z)}. \tag{40}$$

Correspondingly, one expects that the only dimensionless parameter that governs the turbulent statistics in this region should be the ratio of the outer scale of turbulence, ℓ, to the local Monin-Obukhov length-scale Λ, i.e. ℓ/Λ. To see this we will introduce two set of objects. The first set is "‡-objects" which are differ from wall-normalized $^+$ objects, by replacement of the wall fluxes τ_* and F_* by their local, z-dependent, counterparts $-\tau_{xz}(z)$ and $-F_z(z)$:

$$\tau_{ij}^\ddagger \equiv -\frac{\tau_{ij}}{\tau_{xz}} = -\frac{\tau_{ij}^+}{\tau_{xz}^+} = \frac{\tau_{ij}^+}{f_1} \quad\Rightarrow\quad \tau_{xz}^\ddagger = -1, \tag{41a}$$

$$F_i^\ddagger \equiv -\frac{F_i}{F_z} = -\frac{F_i^+}{F_z^+} = \frac{F_i^+}{f_2} \quad\Rightarrow\quad F_z^\ddagger = -1, \tag{41b}$$

$$E_{\mathrm{K}}^{\ddagger} \equiv -\frac{E_{\mathrm{K}}}{\tau_{xz}} = \frac{E_{\mathrm{K}}^{+}}{f_1}, \quad E_{\theta}^{\ddagger} \equiv -E_{\theta}\,\frac{\tau_{xz}}{F_z^2} = E_{\theta}^{+}\,\frac{f_1}{f_2^2}, \tag{41c}$$

$$S_U^{\ddagger} = \frac{S_U\,\nu}{-\tau_{xz}} = \frac{S_U^{+}}{f_1}, \quad S_{\Theta}^{\ddagger} = \frac{S_{\Theta}\,\nu}{-F_z} = \frac{S_{\Theta}^{+}}{f_2}, \tag{41d}$$

$$\ell^{\ddagger} = \frac{\ell\sqrt{-\tau_{xz}}}{\nu} = \ell^{+}\sqrt{f_1}, \quad L^{\ddagger} = L^{+}\sqrt{f_1}, \quad \Lambda^{\ddagger} = L^{\ddagger}\frac{f_1 2}{f_2}. \tag{41e}$$

Correspondingly, in case when $f_1 = f_2 = 1$ the ‡ objects coincide with the $^{+}$ objects.

The second set is two objects, denoted as $S_{U\Lambda}^{\ddagger}$ and $S_{\Theta\Lambda}^{\ddagger}$, that differ from $S_U^{\ddagger}$ and $S_{\Theta}^{\ddagger}$ on multiplication by $\Lambda^{\ddagger}$. Having in mind that $S_U\,\Lambda$ and $S_{\Theta}\,\Lambda$ have dimensionality of velocity and temperature we can define these two objects in a few equivalent ways:

$$S_{U\Lambda}^{\ddagger} \equiv S_U^{\ddagger}\,\Lambda^{\ddagger} = \frac{S_U^{+}\Lambda^{+}}{\sqrt{-\tau_{xz}^{+}}} = \frac{S_U^{+}\Lambda^{+}}{\sqrt{f_1}} = \frac{S_U\,\Lambda}{\sqrt{-\tau_{xz}}}, \tag{41f}$$

$$S_{\Theta\Lambda}^{\ddagger} \equiv S_{\Theta}^{\ddagger}\,\Lambda^{\ddagger} = \frac{S_{\Theta}^{+}\Lambda^{+}\sqrt{-\tau_{xz}^{+}}}{-F_z^{+}} = \frac{S_{\Theta}^{+}\Lambda^{+}\sqrt{f_1}}{f_2} = \frac{S_{\Theta}\,\Lambda\sqrt{-\tau_{xz}}}{-F_z}. \tag{41g}$$

In notations (41) one rewrites the balance Eq. 37 as follows:

$$\tau_{xx}^{\ddagger} = E_{\mathrm{K}}^{\ddagger} - \frac{F_z^{\ddagger}}{2c_{uu}\sqrt{E_{\mathrm{K}}^{\ddagger}}}\frac{\ell}{\Lambda}, \tag{42a}$$

$$\tau_{yy}^{\ddagger} = E_{\mathrm{K}}^{\ddagger}/2, \tag{42b}$$

$$\tau_{zz}^{\ddagger} = \frac{E_{\mathrm{K}}^{\ddagger}}{2} + \frac{F_z^{\ddagger}}{2c_{uu}\sqrt{E_{\mathrm{K}}^{\ddagger}}}\frac{\ell}{\Lambda}, \tag{42c}$$

$$c_{uu}E_{\mathrm{K}}^{\ddagger\,3/2} = \left(F_z^{\ddagger} - \tau_{xz}^{\ddagger}S_{U\Lambda}^{\ddagger}\right)\ell/\Lambda, \tag{42d}$$

$$4\,\widetilde{C}_{\mathrm{RI}}\,c_{uu}\sqrt{E_{\mathrm{K}}^{\ddagger}}\,\tau_{xz}^{\ddagger} = \left(F_x^{\ddagger} - \tau_{zz}^{\ddagger}\,S_{U\Lambda}^{\ddagger}\right)\ell/\Lambda, \tag{42e}$$

$$C_{\theta\theta}\,c_{uu}\sqrt{E_{\mathrm{K}}^{\ddagger}}\,E_{\theta}^{\ddagger} = -F_z^{\ddagger}\,S_{\Theta\Lambda}^{\ddagger}\,\ell/\Lambda, \tag{42f}$$

$$C_{u\theta}\,c_{uu}\sqrt{E_{\mathrm{K}}^{\ddagger}}\,F_x^{\ddagger} = -\left(\tau_{xz}^{\ddagger}S_{\Theta\Lambda}^{\ddagger} + C_{\mathrm{SU}}F_z^{\ddagger}\,S_{U\Lambda}^{\ddagger}\right)\ell/\Lambda, \tag{42g}$$

$$C_{u\theta}\,c_{uu}\sqrt{E_{\mathrm{K}}^{\ddagger}}\,F_z^{\ddagger} = -\left(\tau_{zz}^{\ddagger}S_{\Theta\Lambda}^{\ddagger} + 2\,C_{\mathrm{E}\Theta}\,E_{\theta}^{\ddagger}\right)\ell/\Lambda, \tag{42h}$$

$$\tau_{xz}^{\ddagger} = -1, \qquad F_z^{\ddagger} = -1. \tag{42i}$$

These equations are the main result of current Sect. 3. They may be considered as a "Minimal Model" for stably stratified TBL, that respects the conservation of energy, describes anisotropy of turbulence and all relevant fluxes explicitly and, nevertheless is still simple enough to allow comprehensive analytical analysis, that results in an approximate analytical solution (with reasonable accuracy) for the mean velocity and temperature gradients S_{U} and S_{Θ}, and all second-order (cross)-correlation functions.

As expected, the only parameter appearing in the Minimal Model (42) is ℓ/Λ. The outer scale of turbulence, ℓ, does not appear by itself, only via the ratio ℓ/Λ. Therefore our goal now is to solve Eq. 42 in order to find five functions of only one argument ℓ/Λ: $S_{U\Lambda}^{\ddagger}$, $S_{\Theta\Lambda}^{\ddagger}$,

$E_{\mathrm{K}}^{\ddagger}$, $E_{\theta}^{\ddagger}$ and $F_{x}^{\ddagger}$. After that we can specify the dependence $\ell^{\ddagger}(z^{\ddagger})$ and then reconstruct the z-dependence of these five objects.

4 Results and discussion

4.1 Analytical solution of the Minimal-Model balance Eq. 42

This subsection is devoted to an analytical and numerical analysis of the Minimal-Model (42). An example of numerical solution of Eq. 42 [with some reasonable choice of the phenomenological parameters (44)] is shown in Fig. 1. Nevertheless, it would be much more instructive to have approximate analytical solutions for all correlations that will describe their ℓ/Λ-dependence with reasonable accuracy. The detailed procedure of finding these solutions is simple but rather cumbersome. A brief overview is as follows.

The Eq. 42 can be reformulated as a polynomial equation of ninth order for the only unknown $\sqrt{E_{\mathrm{K}}^{\ddagger}}$. An analysis of its structure helps to formulate an effective interpolation formula (43), discussed below. Hence, we found the solutions of Eq. 42 at neutral stratification, $\ell/\Lambda = 0$, corrected up to the linear order in ℓ/Λ. Its comparison with the existing DNS data resulted in an estimate for the constants $\widetilde{C}_{\mathrm{RI}} \approx 1.46$, and $c_{uu} \approx 0.36$. Then, we considered the region $\ell/\Lambda \to \infty$. Even though such a condition may not be realizable in nature, from a methodological point of view, as we will see below, it enables to obtain the desired analytical approximation. The $\ell/\Lambda \to \infty$ asymptotic solution with corrections, linear in the small parameter $(\ell/\Lambda)^{-4/3}$, were found. Now we are armed to suggest an interpolation formula:

$$c_{uu} E_{\mathrm{K}}^{\ddagger 3/2}\,(\ell/\Lambda) \simeq \frac{11}{3}\frac{\ell}{\Lambda} + \left[\kappa\sqrt{1+\left(\frac{11}{3}\kappa\frac{\ell}{\Lambda}\right)^{2/3}}\right]^{-1}, \tag{43a}$$

where κ is is the von-Kármán constant. This formula coincides with the exact solutions for $\ell/\Lambda = 0$ and for $\ell/\Lambda \to \infty$, including the leading corrections to both asymptotics. Moreover, in the region $\ell/\Lambda \sim 1$, Eq. 43a accounts for the structure of the exact polynomial. As a result, the interpolation formula (43a) is close to the numerical solution with deviations smaller than 3% in the entire region $0 \le \ell/\Lambda < \infty$, see left middle panel in Fig. 1. Together with Eq. 42d it produces a solution for $S_{U}^{\ddagger}$, that can be written as

$$S_{U}^{\ddagger}(\ell^{\ddagger}) \simeq \left(\lambda_1^{\ddagger}\right)^{-1} + \left[\kappa\,\ell^{\ddagger}\sqrt{1+(\ell^{\ddagger}/\lambda_2^{\ddagger})^{2/3}}\right]^{-1}, \tag{43b}$$

where $\lambda_1^{\ddagger} \equiv 3\Lambda^{\ddagger}/14$, $\lambda_2^{\ddagger} \equiv 3\Lambda^{\ddagger}/11\kappa$. This formula gives the same accuracy $\sim 3\%$, see left upper panel in Fig. 1. We demonstrate below that the proposed interpolation formulae describe the ℓ/Λ-dependence of the correlations with a very reasonable accuracy, about 10%, for any $0 \le \ell/\Lambda < \infty$, see black dashed lines in Fig. 1.

Unfortunately, a direct substitution of the interpolation formula (43) into the exact relation for $S_{\Theta\Lambda}^{\ddagger}$ obtained from the system (42) works well only for small ℓ/Λ, in spite of the fact that the interpolation formula is rather accurate in the whole region. We need therefore to derive an independent interpolation formula for $S_{\Theta}^{\ddagger}$. Using expansions for small $\ell/\Lambda \ll 1$ and large $\ell/\Lambda \gg 1$ we suggest

$$S_{\Theta}^{\ddagger}(\ell^{\ddagger}) \simeq S_{\Theta}^{\ddagger\infty} + \frac{S_{\Theta,0}^{\ddagger} + 6(c_{uu}\alpha)^{4/3} S_{\Theta,1}^{\ddagger\infty}}{\left(1+\alpha\,\ell^{\ddagger}/\Lambda^{\ddagger}\right)^{4/3}}, \tag{43c}$$

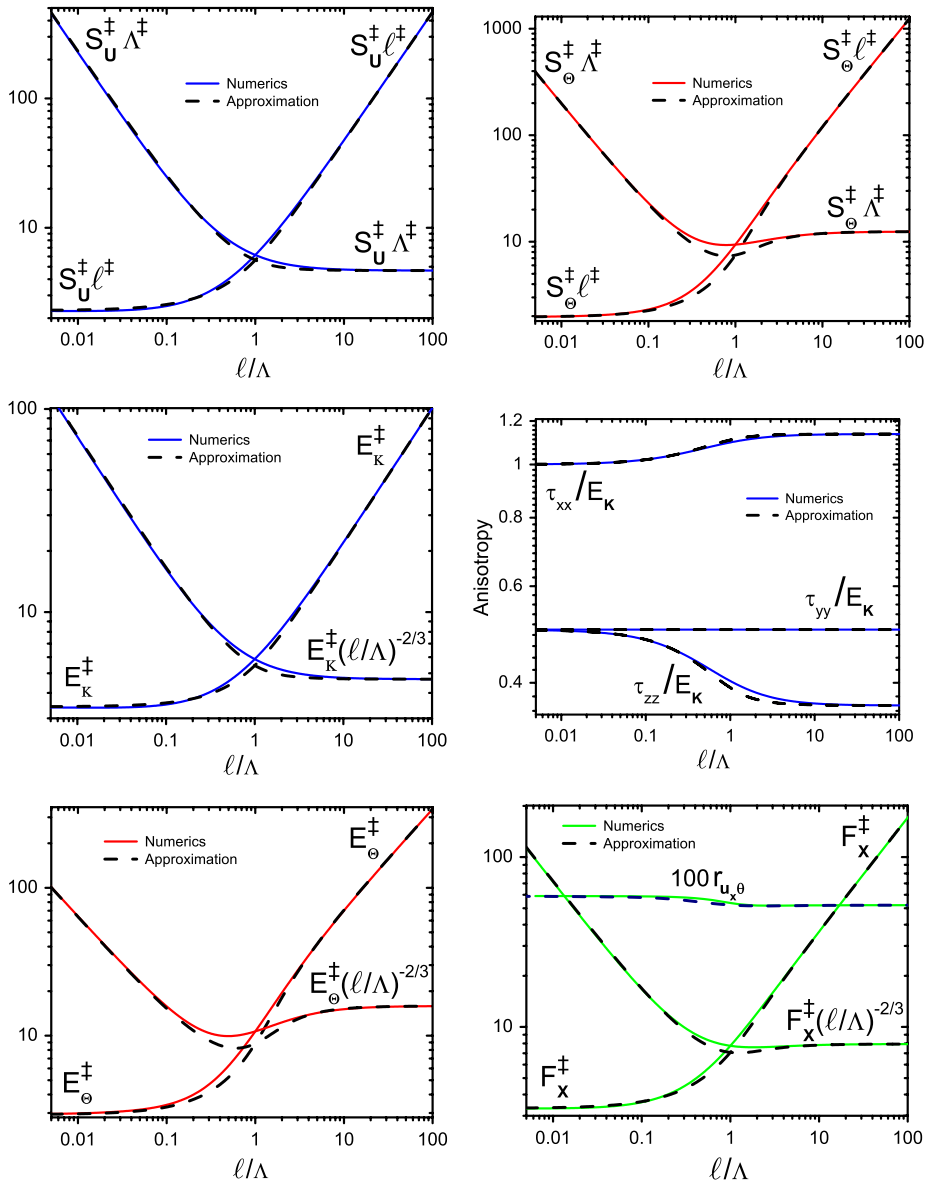

Fig. 1 Log–log plots of the normalized velocity mean shears $S_{\mathrm{U}}^{\ddagger}\ell^{\ddagger}$ and $S_{\mathrm{U}}^{\ddagger}\Lambda^{\ddagger}$ (left upper panel), normalized mean-temperature gradients $S_{\Theta}^{\ddagger}\ell^{\ddagger}$ and $S_{\Theta}^{\ddagger}\Lambda^{\ddagger}$ (right upper panel), the turbulent kinetic energy $E_{\mathrm{K}}^{\ddagger}$ and $E_{\mathrm{K}}^{\ddagger}(\ell/\Lambda)^{-2/3}$ (left middle panel), partial kinetic energies τ_{ii}/E_{K} (right middle panel), temperature energy $E_{\theta}^{\ddagger}$ and $E_{\theta}^{\ddagger}(\ell/\Lambda)^{-2/3}$ (left lower panel) and horizontal thermal flux $F_x^{\ddagger}$ and $F_x^{\ddagger}(\ell/\Lambda)^{-2/3}$ (right lower panel) versus ℓ/Λ. Here we also show normalized correlation function $r_{u\theta} \equiv \langle u_x\theta\rangle/\sqrt{\langle u_x^2\rangle\langle\theta^2\rangle} = F_x/\sqrt{2\,\tau_{xx}E_\theta}$. Red, blue and green solid lines—exact numerical solutions before and after normalization by the large ℓ/Λ asymptotics, black dashed and dot-dashed lines—approximate analytical solutions. The region $\ell > L$ may not be realized in the Nature. In this case it has only methodological character

in which

$$S^{\ddagger}_{\Theta,0} = 2^{1/4} c_{uu} C_{U\Theta} / \widetilde{C}^{1/4}_{RI} \ell^{\ddagger}, \quad S^{\ddagger\infty}_{\Theta} = -14(C_{SU} - 4C_{U\Theta}/3)/3\Lambda^{\ddagger},$$
$$S^{\ddagger\infty}_{\Theta,1} = -C_{u\theta}(2\widetilde{C}_{RI} - (11\, C_{u\theta} - 3\, C_{SU})/3\, S^{\ddagger\infty}_{\Theta}\Lambda^{\ddagger})/\Lambda^{\ddagger},$$

and α satisfies

$$S^{\ddagger}_{\Theta,1}\ell^{\ddagger} = S^{\ddagger\infty}_{\Theta}\Lambda^{\ddagger} + 6\, S^{\ddagger\infty}_{\Theta,1}\, \Lambda^{\ddagger}(c_{uu}\alpha)^{4/3} - 4\alpha S^{\ddagger}_{\Theta,0}/3,$$
$$S^{\ddagger}_{\Theta,1}\ell^{\ddagger} = -C_{u\theta}\left(3/4\widetilde{C}_{RI} - 22 + 3C_{SU}/C_{u\theta}\right)/24\widetilde{C}_{RI}.$$

Equation 43c is constructed such that the leading and sub-leading asymptotics for small and large ℓ/Λ coincide with the first two terms in the exact expansions at "almost" neural stratification and extremely strong stratification. As a result, Eq. 43c approximates the exact solution with errors smaller then 5% for $\ell/\Lambda < 1$ and $\ell/\Lambda > 50$ and with errors smaller than 10% for any ℓ/Λ, see right upper panel in Fig. 1.

Substituting the approximate Eq. 43 into the exact relations (42), one gets approximate solutions $E^{\ddagger}_{\theta}$ and $F^{\ddagger}_{x}$ with errors smaller than 10%, see lower panels in Fig. 1. All the actual values of constants used in final computations are summarized here:

$$c_{uu} \simeq 3.42^{-3/2}/\kappa, \quad \widetilde{C}_{RI} \simeq 3.42^{2}/8, \quad C_{E\theta} \simeq -2/3, \quad C_{\theta\theta} \simeq 1, \quad C_{SU} \simeq 5.6, \quad C_{U\theta} \simeq 5,$$
$$\kappa \simeq 0.436. \tag{44}$$

Using relationships (41) one can represent Eq. 43 in traditional wall normalization. For example, Eq. 43b can be rewritten as

$$S^{+}_{U}(\ell^{+}) \simeq \sqrt{f_1}\left\{\left(\lambda^{+}_{1}\right)^{-1} + \left[\kappa\, \ell^{+}\sqrt{1 + \left(\ell^{+}/\lambda^{+}_{2}\right)^{2/3}}\right]^{-1}\right\}, \tag{45}$$

where $\lambda^{+}_{1} \equiv 3L^{+} f_1^{3/2}/14 f_2$, $\lambda^{+}_{2} \equiv 3L^{+} f_1^{3/2}/11 f_2 \kappa$.

4.2 Mean velocity and temperature profiles

In principle, integrating the mean shear S^{+}_{U} and the mean temperature gradient S^{+}_{Θ}, one can find the mean velocity and temperature profiles. Unfortunately, to do so we need to know S^{+}_{U} and S^{+}_{Θ} as functions of the elevation z, while in our approach they are found as functions of $\ell(z)/\Lambda(z)$ also involving fluxes parametrization functions $f_1(z)$ and $f_2(z)$. Important that the outer scale of turbulence $\ell(z)$ and local Monin-Obukhov length $\Lambda(z)$ are external parameters of the problem that have to be found separately.

The importance of an accounting for the proper physically motivated dependance of ℓ on z for an example of channels and pipes has been recently shown by [32]. As for the problem at hands, for small elevations with respect to the Monin-Obukhov length $L \equiv \Lambda(0)$, i.e. for $z \ll L$, it is well accepted that $\ell(z)$ is proportional to z, while the $\ell(z)$ dependence is still under debate for z comparable or exceeding L. For $z \sim L$ the assignment and discussion of the actual dependence of the outer scale of turbulence, $\ell(z)$, which is manifested in Nature is out of the scope of this paper, and is remained for future work. At time being, we can analyze consequences of our approach for the following versions of $\ell(z)$ dependence at $z \gg L$:

- function $\ell(z)$ is saturated at some level of the order of L. For concreteness we can take

$$1/\ell(z) = \sqrt{(d_1 z)^{-2} + (d_2 L)^{-2}}, \quad d_1 \sim d_2 \sim 1. \tag{46}$$

- $\ell(z)$ is again proportional to z for elevations much larger than L: $\ell(z) = d_3 z$ but with the small proportionality constant $d_3 < d_1$. If so, we can also study the case $\ell(z) \gg L$ even though such a condition may not be realizable in Nature. In that case our analysis of the limit $\ell(z) \gg L$ has only a methodological character: it allows to derive an approximate analytic solution for all the objects of interest that is also valid for the outer scale of turbulence not exceeding a value of the order of L.

Analytical treatments become more simple near the ground, where one can neglect the variations of fluxes, using approximation of "constant flux layer": $f_1(z) = f_2(z) = 1$. In this case Λ becomes L, and all ‡ objects are transformed into $^+$ ones. The resulting plots of U^+ in this approximation are shown on Fig. 2, upper panel. Even taking $\ell(z) = z$ one gets a very similar velocity profile, see Fig. 2, lower panel. With $\ell(z) = z$ we found an analytical expression for the mean-velocity profile using the interpolation Eq. 43b for S_U^+:

$$U^+(z) = \frac{1}{\kappa} \ln \left[\frac{z}{z_{u0} \left(1 + \sqrt{1 + (z/L_2)^{2/3}} \right)^3} \right] + \frac{z}{L_1}. \tag{47}$$

Here z_{u0} is the roughness length, $L_1^+ \equiv 3L^+/14$, $L_2^+ \equiv 3L^+ \big/ 11\kappa$.

The resulting mean velocity profiles have logarithmic asymptotic for zL in agreement with meteorological observations. Usually the observations are parameterized by a so-called log-linear approximation [31]:

$$U^+ = \kappa^{-1} \ln(z/z_{u0}) + z/L_1, \tag{48a}$$

which is plotted in Fig. 2 by dotted lines. One sees some deviation in the region of intermediate z. The reason is that the real profile [see, e.g. Eq. 47] has a logarithmic term that saturates for $z \gg L$, while in the approximation (48a) this term continues to grow. To fix this one can use Eq. 47 (with $L_2 = L_1$ for simplicity), or even its simplified version

$$U^+ = \frac{1}{\kappa} \ln \frac{z}{z_{u0} \sqrt{1 + (z/L_1)^2}} + \frac{z}{L_1}. \tag{48b}$$

This approximation is plotted as a dashed line on Fig. 2 for comparison.

The temperature profiles in our approach look similar to the velocity ones, see Fig. 2, lower panel. They have logarithmic asymptotic for $\ell < L$ and linear behavior for $\ell > L$. Correspondingly, they can be fitted by a log-linear approximation, like (48a), or even better, by an improved version of it, like Eq. 48b. Clearly, the values of constants will be different: $\kappa \Rightarrow \kappa_T$, $L_1 \Rightarrow L_{1,T}$, etc.

4.3 Profiles of second-order correlations

The computed profiles of the locally scaled turbulent kinetic and temperature energies, horizontal thermal flux profile and the anisotropy profiles are shown on Fig. 1 in the middle and lower panels.

The profiles of $E_K^\ddagger$ (left middle panel) and of $E_\Theta^\ddagger$ and $F_x^\ddagger$ (lower panels), that are $\propto (\ell/\Lambda)^{2/3}$ for $\ell \gg \Lambda$ (if realizable). With the interpolation formula (46), the profiles of the second order correlations have to saturate at levels corresponding to $\ell \simeq L$. This sensitivity to the z-dependence of $\ell(z)$ makes a comparison of the prediction with experimental data very desirable.

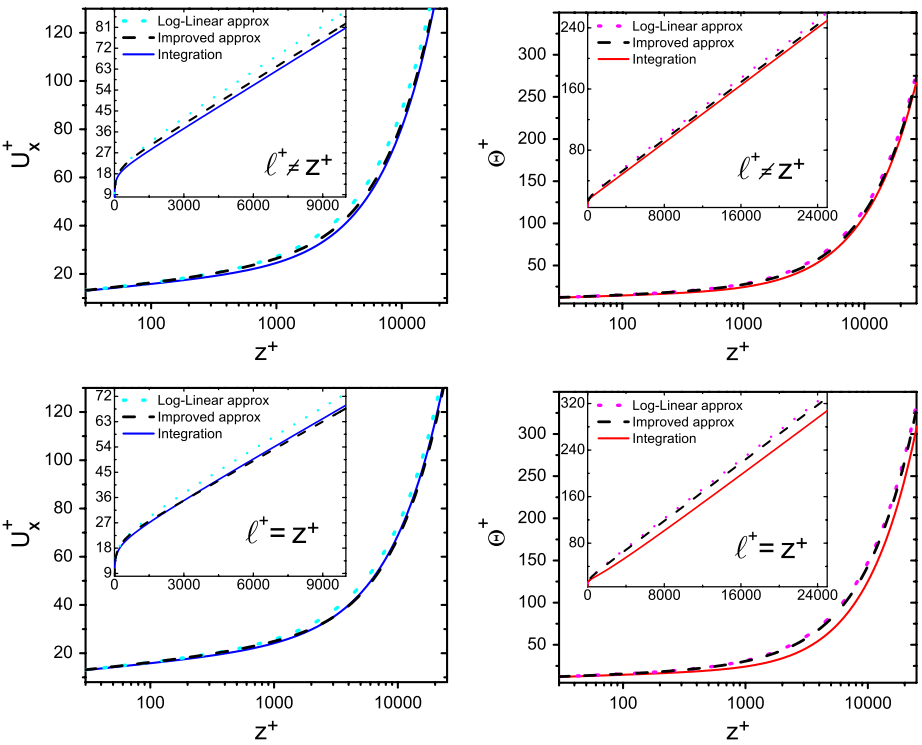

Fig. 2 Computed with Eq. 46 (for $d_1 = d_2 = f_1(z) = f_2(z) = 1$) plots of U^+ (blue solid lines on left panels) and Θ^+ (red solid lines on right panels) versus z^+ for $L^+ = 1000$. In upper panels $\ell(z)$ is taken from Eq. 46, while in lower panels $\ell(z) = z$. Log-linear approximation (48a) to all profiles is shown by dotted lines, its improved version (48b) by dashed lines. The region $\ell > L$ may not be realized in the Nature. In this case it has only methodological character

4.4 Turbulent transport, Richardson and Prandtl numbers

In our notations the turbulent viscosity and thermal conductivity, turbulent Prandtl number, the gradient- and flux-Richardson numbers are

$$\nu_{\mathrm{T}}^+ \equiv -\frac{\tau_{xz}^+}{S_{\mathrm{U}}^+} = \frac{1}{S_{\mathrm{U}}^\ddagger} \equiv C_\nu(\ell/\Lambda)\frac{\tau_{zz}^\ddagger}{\gamma_{uu}^\ddagger}, \tag{49a}$$

$$\chi_{\mathrm{T}}^+ \equiv -\frac{F_z}{S_\Theta} = \frac{1}{S_\Theta^\ddagger} \equiv C_\chi(\ell/\Lambda)\frac{\tau_{zz}^\ddagger}{\gamma_{uu}^\ddagger}, \tag{49b}$$

$$\mathrm{Pr}_{\mathrm{T}} \equiv \nu_{\mathrm{T}}/\chi_{\mathrm{T}} = S_\Theta^\ddagger/S_U^\ddagger, \tag{49c}$$

$$\mathrm{Ri}_{\mathrm{grad}} \equiv \frac{\beta S_\Theta}{S_U^2} = \frac{S_\Theta^\ddagger}{\Lambda^\ddagger S_U^{\ddagger 2}} = \frac{\ell}{\Lambda}\frac{S_{\Theta\ell}^\ddagger}{S_{U\ell}^{\ddagger 2}}, \tag{49d}$$

$$\mathrm{Ri}_{\mathrm{flux}} \equiv \frac{\beta F_z}{\tau_{xy} S_U} = \frac{1}{\Lambda^\ddagger S_U^\ddagger} = \frac{\ell}{\Lambda}\frac{1}{S_{U\ell}^\ddagger}, \tag{49e}$$

$$\mathrm{Ri}_{\mathrm{grad}} = \mathrm{Ri}_{\mathrm{flux}}\,\mathrm{Pr}_{\mathrm{T}}. \tag{49f}$$

With Eqs. 49a and 49b we introduce also two dimensionless functions $C_\nu(\ell/\Lambda)$ and $C_\chi(\ell/\Lambda)$ that are taken as constants in the down-gradient transport approximation (2) described in the Introduction.

4.4.1 Locally scaled momentum and heat diffusivities

It is tempting to compare the model predictions with proper experimental observations and results of numerical simulations, which presumably involve less assumptions and approximations that the model itself. To demonstrate the situation with such a comparison for stable stratified TBL we plot together Nieuwstadt experimental observations [10] and the model results for the so-called locally scaled momentum and heat diffusivities defined below. The definitions of the parameters is taken from [10] and interpreted in terms of the model at hands. Hence, the effective diffusivities of momentum (K_M) and heat (K_H) are just:

$$K_\mathrm{M} \equiv -\tau_{xz}/S_\mathrm{U} = \nu_\mathrm{T}, \quad \text{and} \quad K_\mathrm{H} \equiv -F_z/S_\Theta = \chi_\mathrm{T}, \tag{50}$$

while the (Nieuwstadt's) local Monin-Obukhov length in our case is Λ/κ. Thus, the non-dimensionalised locally scaled momentum and heat diffusivities become:

$$\phi_\mathrm{KM}(\zeta) \equiv \frac{\kappa K_\mathrm{M}}{\Lambda\sqrt{-\tau_{xz}}} = \frac{\kappa}{S_\mathrm{U}^\ddagger \Lambda^\ddagger}, \quad \phi_\mathrm{KH}(\zeta) \equiv \frac{\kappa K_\mathrm{H}}{\Lambda\sqrt{-\tau_{xz}}} = \frac{\kappa}{S_\Theta^\ddagger \Lambda^\ddagger}, \quad \zeta = \kappa\frac{z}{\Lambda}, \tag{51}$$

and we assumed $\ell(z) = z$. It is a simple exercise to write down approximate analytical formulae for ϕ_KM and ϕ_KH just by using Eqs. 43b and 43c. The plots of ϕ_KM and ϕ_KH versus z/Λ are depicted in Fig. 3. For this set of plots, the von-Kármánconstant was chosen to be the same as in [33], i.e. $\kappa = 0.4$, which is on 0.05 larger than in [10]. One sees that the observational data have quite large error bars originated from variations in weather conditions.

Notice, that various versions of LES also differ significantly having problems, for example, with non-dimensional gradients near the surface at the first few comutational levels. Nevertheless for completeness we present in Fig. 3 also LES from GABLS at finest resolution of 2 m [33]. The model predictions (thick lines) lay inside the region confined by the observations and LES.

As an example of another comparison with experimental observations we consider the normalized cross-correlation function $r_{u\theta} \equiv \langle u_x\theta\rangle/\sqrt{\langle u_x^2\rangle\langle\theta^2\rangle} = F_x/\sqrt{2\,\tau_{xx}E_\theta}$. According

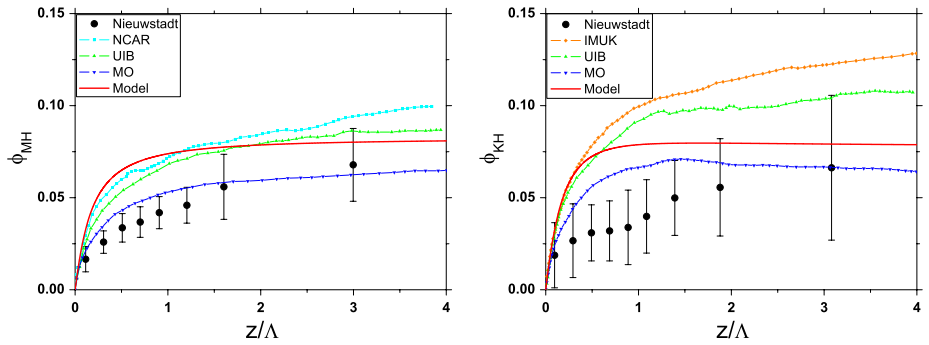

Fig. 3 Locally scaled momentum (left) and heat (right) diffusivities. Circles (together with the standard deviation bars)—Nieuwstadt experimental observations [10], joined symbols—LES data from GABLS at finest resolution of 2 m (see for details [33]), thick solid line—the model results

to observations by Basu et al. [34], it is more or less a constant about 0.5 for z/Λ in the range $0 \div 1$. For the current choice of fitting parameters (44), our model gives the constant of about 0.9. Reducing the fitting parameter C_{SU} twice results in the constant level, which lies in between 0.5 and 0.6 as it is shown in Fig. 1, lower right panel. Nevertheless we do not think that the quantitative agreement of the model with observation and LES means much. At the present quality of the observations and simulations for us much more important the self-consistency and elegance of the model rather than a comparison with currently available data.

4.4.2 Approximation of down-gradient transport and its violation in stably stratified TBL

As we mentioned in the Introduction, the concept of the down-gradient transport assumes that the momentum and thermal fluxes are proportional to the mean velocity and temperature gradients, see Eq. 2:

$$\tau_{xz} = -\nu_{\mathrm{T}} S_U, \quad F_z = -\chi_{\mathrm{T}} S_\Theta, \tag{52}$$

where ν_{T} and χ_{T} are effective turbulent viscosity and thermal conductivity, that can be estimated by dimensional reasoning. Equation 2, giving this estimates, include additional physical arguments that vertical transport parameters should be estimated via vertical turbulent velocity, $\sqrt{\tau_{zz}}$, and characteristic vertical scale of turbulence, ℓ_z. The relations between the scales ℓ_j in different j-directions in anisotropic turbulence can be found in the approximation of time-isotropy, according to which

$$\frac{\sqrt{\tau_{xx}}}{\ell_x} = \frac{\sqrt{\tau_{yy}}}{\ell_y} = \frac{\sqrt{\tau_{zz}}}{\ell_z} \equiv \gamma \Rightarrow \gamma_{uu}. \tag{53}$$

Here γ is a characteristic isotropic frequency of turbulence, that for concreteness can be taken as the kinetic energy relaxation frequency γ_{uu}. The approximation (53) is supported by experimental data, according to which in anisotropic turbulence the ratios ℓ_i/ℓ_j $(i \neq j)$ are larger then the ratios $\ell_i \sqrt{\tau_{jj}}/\ell_j \sqrt{\tau_{ii}}$ that are close to unity. With this approximations ν_{T} and χ_{T} can be estimated as follows:

$$\nu_{\mathrm{T}} = C_\nu \tau_{zz}/\gamma_{uu}, \quad \chi_{\mathrm{T}} = C_\chi \tau_{zz}/\gamma_{uu}, \tag{54}$$

where, according to the approximation of down-gradient transport, the dimensionless parameters C_ν and C_χ are taken as constants, independent of the level of stratification.

In order to check how the approximation (52, 54) works in the stratified TBL for both fluxes, one can consider Eq. 52 as *definitions* of ν_{T} and χ_{T} and Eq. 54 as *definitions* of C_ν and C_χ. This gives

$$C_\nu \equiv -\frac{\tau_{xz}}{\tau_{zz}} \frac{\gamma_{uu}}{S_U} = \frac{\gamma_{uu}^{\ddagger}}{S_U^{\ddagger} \tau_{zz}^{\ddagger}}, \quad C_\chi \equiv -\frac{F_x}{\tau_{zz}} \frac{\gamma_{uu}}{S_\Theta} = \frac{\gamma_{uu}^{\ddagger}}{S_\Theta^{\ddagger} \tau_{zz}^{\ddagger}}. \tag{55}$$

Recall, that in this paper the down-gradient approximation is not used at all. Instead, we are using exact balance equations for all relevant second order correlations, including τ_{xz} and F_x. Substituting our results in the RHS of the definitions (55) we can find, how C_ν and C_χ depend on ℓ/Λ that determines the level of stratification in our approach.

The resulting plots of the ratios $C_\nu(\ell/\Lambda)/C_\nu(0)$ and $C_\chi(\ell/\Lambda)/C_\chi(0)$ are shown in the left-upper panel in Fig. 4. One sees that the $C_\nu(\ell/\Lambda)$ and $C_\chi(\ell/\Lambda)$ can be considered approximately as constants only for $\ell \leq 0.2\,\Lambda$. For larger ℓ/Λ both C_ν and C_χ rapidly decrease,

more or less in the same manner, diminishing by an order of magnitude already for $\ell \approx 2\,\Lambda$. For larger ℓ/Λ one can use the asymptotic solution for $\ell \gg \Lambda$ according to which

$$S_U^{\ddagger}, S_\Theta^{\ddagger} \simeq 1/\Lambda^{\ddagger}, \quad \gamma_{uu}^{\ddagger} \simeq \sqrt{E_{\rm K}^{\ddagger}}\,/\ell^{\ddagger} \simeq (\ell/\Lambda)^{1/3}\,/\ell^{\ddagger}\,, \quad \tau_{zz}^{\ddagger} \simeq (\ell/\Lambda)^{2/3}. \tag{56}$$

This means that both functions vanish as $(\ell/\Lambda)^{-4/3}$:

$$C_\nu \simeq 0.01\,(\ell/\Lambda)^{-4/3}\,, \quad C_\chi \simeq 0.003\,(\ell/\Lambda)^{-4/3}\,, \tag{57}$$

where numerical prefactors account for the accepted values of the dimensionless fit parameters.

The physical reason for the strong dependence of C_ν and C_χ on stratification is as follows: in the RHS of Eq. 34e for the momentum flux and Eq. 35b for the vertical heat flux there are two terms. The first ones, proportional to τ_{zz} and velocity (or temperature) gradients correspond to the approximation (52), giving (in our notations) $C_\nu = \text{const}$ and $C_\chi = \text{const}$, in agreement with the down-gradient transport concept. However, there are second contributions to the vertical momentum flux $\propto F_x$ and to the vertical heat flux, that is proportional to βE_θ. In our approach both contributions are negative, giving rise to the *counter-gradient fluxes*. What follows from our approach, is that these counter-gradient fluxes cancel (to the leading order) the down-gradient contributions in the limit $\ell/\Lambda \to \infty$. As a result, in this limit the effective turbulent diffusion and thermal conductivity vanish, making the down-gradient approximation for them (with constant C_ν and C_χ) irrelevant even qualitatively for $\ell > \Lambda$.

In our picture of stable temperature-stratified TBL, the turbulence exists at any elevations, where one can neglect the Coriolis force. Moreover, the turbulent kinetic and temperature energies increase as $(\ell/\Lambda)^{2/3}$ for $\ell > \Lambda$, see left middle and lower panels in Fig. 1. At the same time, the mean velocity and potential temperature change the (ℓ/L)-dependence from logarithmic lo linear, see Fig. 2 and (modified) log-linear interpolation formula (48b). Correspondingly, the shear of the mean velocity and *the mean temperature gradient* saturate at some elevation (and at some ℓ/L), and $\mathrm{Ri}_{\rm grad}$ *saturates as well*. This predictions agree with large eddy simulation by [35], see Fig. 5 in [9], where $\mathrm{Ri}_{\rm grad}$ can be considered as saturating around 0.4 for $z/L \approx 100$.

Nevertheless, our analytical result of saturating $\mathrm{Ri}_{\rm grad}$ disagree with various observational, experimental and numerical data, collected in Ref. [9], see Figs. 1, 2, upper panel of Figs. 3 and 4, where various data are plotted as functions of the gradient Richardson number in the interval (0, 100). The conditions at which these data were obtained do not correspond to the situation considered in our paper.

Notice that the turbulent closures of kind used above cannot be applied for strongly stratified flows with $\mathrm{Ri}_{\rm grad} > 1$ (may be even at $\mathrm{Ri}_{\rm grad} \sim 1$). There are two reasons for that. The first one was mentioned in the Introduction. Namely, for $\mathrm{Ri}_{\rm grad} > 1$ the Brunt-Väisälä frequency $N \equiv \sqrt{\beta S_\Theta}$, is larger then the eddy-turnover frequency and therefore there are weakly decaying Kelvin-Helmoholtz internal gravity waves which, generally speaking, have to be accounted for in the momentum and energy balance equations.

The second reason, that makes the results very sensitive to the contribution of internal waves follows from the fact that vortical turbulent fluxes vanish (at fixed velocity and temperature gradients). Therefore even relatively small contributions of different nature to the momentum and thermal fluxes may be important.

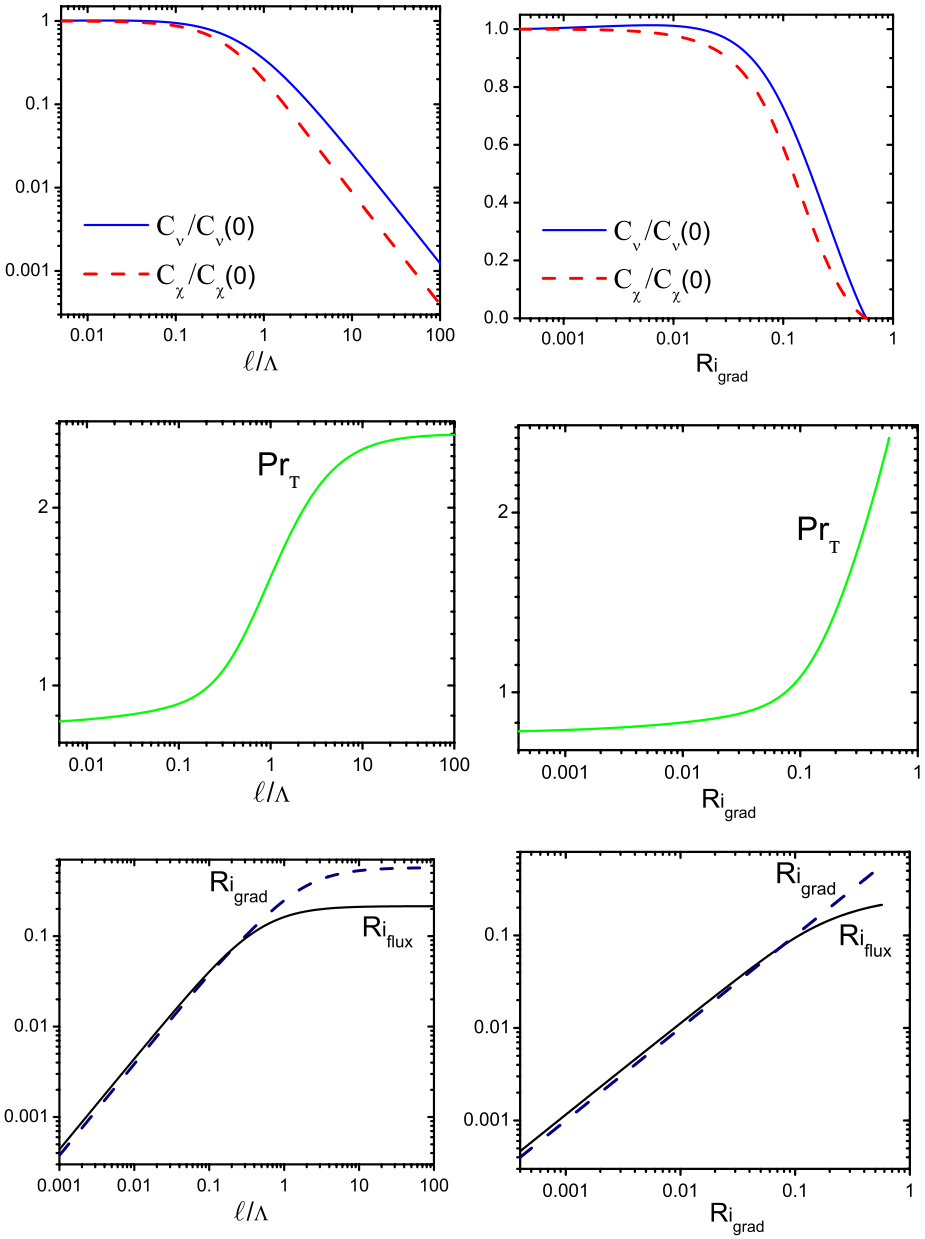

Fig. 4 Log–log plots of "down-gradient coefficient-functions" C_ν (solid blue lines) and C_χ (red dashed lines)—upper panels; turbulent Prandtl number $\mathrm{Pr_T}$ (green lines on middle panels) and $\mathrm{Ri_{flux}}$ (black solid lines), $\mathrm{Ri_{grad}}$ (black dashed lines)—on lower panels as function of ℓ/Λ (left panels) and versus $\mathrm{Ri_{grad}}$ (right panels). Notice, that the presented dependencies have qualitative character, and the choice of constants $C_{...}$ depends on the actual functional form $\ell(z)$. For simplicity, we took $\ell(z) = z$.The region $\ell > L$ may not be realized in the Nature. In this case it has only methodological character

5 Summary

In the paper we address the dynamical and statistical description of stably temperature stratified atmospheric turbulent boundary layer analyzing traditional approaches to this problem, based on the profiles of mean quantities, velocity second-order correlations, and dimensional estimates. In particular we considered the origin of well known difficulty with prediction of the suppression of turbulence at a small critical value of the Richardson number, in contradiction with observations. As a result we present a relatively simple algebraic closure approach, that takes into full account all the second-order statistics, but consider balances of Reynolds stresses and velocity-temperature cross correlations in local approximations. Ideologically our model is quite close to the Nieuwstadt's model [10] and similarly to it expresses mean profiles as functions of the ration of the outer scale of turbulence $\ell(z)$ over the local Monin-Obukhov scale $\Lambda(z)$. We demonstrated explicitly that our model respects the conservation of total mechanical energy and in this sense is a step forward with respect to widely used "down-gradient" approximation (2), in which the dimensionless coefficients C_ν and C_χ are assumed to be (ℓ/Λ)-independent. Our model allows full analytical tractability culminating in an analytic solution of the profiles of all mean quantities and all second-order correlations removing the unphysical predictions of previous theories. We propose that the approach taken here is sufficient to describe the lower parts of the atmospheric boundary layer, as long as the Richardson number does not exceed an order of unity. For much higher Richardson numbers the physics may change qualitatively, requiring careful consideration of the potential Kelvin-Helmoholtz waves and their interaction with the vortical turbulence.

The final conclusion is that the TBL modeling at large level of stratification requires an accounting for turbulence of the internal waves together with the vortical turbulence, and the analysis of available data calls for serious revision. Definitely, new observations, laboratory and numerical experiments with control of internal wave activity are very likely.

Acknowledgements This work has been inspired by discussions with Sergej Zilitinkevich, Tov Elperin, Natan Kleeorin and Igor Rogachevskii, who stressed an importance of the conservation of total mechanical energy of turbulence for the adequate description of stratified TBL. We are grateful to all anonymous referees for their comprehensive reports with numerous critical comments that helped us improve the presentation. This work has been supported by the Transnational Access Programme at RISC-Linz, funded by the European Commission Framework 6 Programme for Integrated Infrastructures Initiatives under the project SCIEnce (Contract No. 026133).

Appendix

On the closure problem of triple correlations via second order correlations

Let us look more carefully at the approximation (36), which is

$$\gamma_{uu} = c_{uu}\sqrt{E_{\rm K}}\,/\ell\ , \quad \gamma_{\rm RI} = C_{\rm RI}\gamma_{uu}, \quad \widetilde{\gamma}_{\rm RI} = \widetilde{C}_{\rm RI}\gamma_{\rm RI}, \quad \gamma_{\theta\theta} = C_{\theta\theta}\gamma_{uu}, \quad \gamma_{\rm RD} = C_{u\theta}\gamma_{uu}. \tag{58}$$

The dimensional reasoning that leads to this approximation is questionable for problems having a dimensionless parameter ℓ/Λ. Generally speaking, all "constants" $c_{...}$ and $C_{...}$ in Eq. 58 can be any functions of ℓ/Λ. Presently we just hope that a possible ℓ/Λ dependence of these functions is relatively weak and does not affect the qualitative picture of the phenomenon.

Moreover, even the assumption (28a) that the dissipation of the thermal flux ε_i is proportional to the thermal flux and the assumption (28b) that the dissipation of E_θ, $\varepsilon \propto E_\theta$ are

also questionable. Formally speaking, one cannot guarantee that the tripple cross-correlator $\langle\theta uu\rangle$ that estimates ε, can be (roughly speaking) decomposed like $\langle u\theta\rangle\sqrt{\langle uu\rangle}$, i.e really proportional to $F = \langle u\theta\rangle$ as it stated in Eq. 28a. Theoretically, one cannot exclude the decomposition $\langle\theta uu\rangle \sim \langle uu\rangle\sqrt{\langle\theta\theta\rangle}$, i.e. a contribution to $\varepsilon \propto E_{\mathrm{K}}$. Similarly, the dissipation ε in the balance (17c) of E_θ, that is determined by the correlator (28b), is $\propto \langle\theta\theta u\rangle$, as it follows from the decomposition $\langle\theta\theta u\rangle \sim \langle\theta\theta\rangle\sqrt{\langle uu\rangle}$ and is stated in Eq. 28b. This correlator allows, for example, the decomposition $\langle\theta\theta u\rangle \sim \langle\theta u\rangle\sqrt{\langle\theta\theta\rangle}$, i.e. contribution to $\varepsilon \propto F$. This discussion demonstrates, that the situation with the dissipation rates is not so simple, as one may think and thus requires careful theoretical analysis that is in our agenda for future work. Our preliminary analysis of this problem shows that all fitting constants are indeed functions of ℓ/Λ. Fortunately, they vary within finite limits in the entire interval $0 \le \ell/\Lambda < \infty$. Therefore we propose that the approximations used in this paper preserve the qualitative picture of the phenomenon. Once again, the traditional down-gradient approximation does not work even qualitatively because corresponding "constants" C_ν and C_χ vanish in the limit $\ell/\Lambda \to \infty$.

References

1. Umlauf L, Burchard H (2005) Second-order turbulence closure models for geophysical boundary layers. A review of recent work. Continent Shelf Res 25:725–827. doi:10.1016/j.csr.2006.02.008
2. Weng W, Taylor P (2003) On modelling the one-dimensional atmospheric boundary layer. Bound Layer Meteorol 107:371–400. doi:10.1023/A:1022126511654
3. Zeman O (1981) Progress in the modeling of planetary boundary layers. Ann Rev Fluid Mech 13:253–272. doi:10.1146/annurev.fl.13.010181.001345
4. Canuto VM (2002) Critical Richardson numbers and gravity waves. Astron Astrophys 384:1119-1123. doi:10.1051/0004-6361:20011773
5. Galperin B, Sukoriansky S, Anderson PS (2007) On the critical Richardson number in stably stratified turbulence. Atm Sci Lett 8(3):65–69. doi:10.1002/asl.153
6. Mellor GL, Yamada T (1974) A hierarchy of turbulence closure models for planetary boundary layer. J Atmos Sci 31:1791–1806. doi:10.1175/1520-0469(1974)031<1791:AHOTCM>2.0.CO;2
7. Richardson LF (1920) The supply of energy from and to atmospheric eddies. Proc. Roy. Soc. London A 97:354–373
8. Richardson LF (1922) Weather prediction by numerical process. Cambridge University Press, xii+236 pp
9. Zilitinkevich SS, Elperin T, Kleeorin N, Rogachevskii I (2007) Energy- and flux-budget (EFB) turbulence closure model for stably stratified flows. Part I: steady-state, homogeneous regimes. Bound Layer Meteorol 125(2):167–191. doi:10.1007/s10546-007-9189-2
10. Nieuwstadt FTM (1984) The turbulent structure of the stable, nocturnal boundary layer. J Atmos Sci 41:2202–2216. doi:10.1175/1520-0469(1984)041<2202:TTSOTS>2.0.CO;2
11. Zilitinkevich SS (2002) Third-order transport due to internal waves and non-local turbulence in the stably stratified surface layer. Q J Royal Meteorol Soc 128:913–925. doi:10.1256/0035900021643746
12. Boussinesq J (1903) The'orique Analytique de la Chaleur, vol 2. Gauthier-Villars, Paris
13. Oberbeck A (1879) Über die Wärmeleitung der Flüssigkeiten bei Berücksichtigung der Strömung infolge Temperaturdifferenzen. Ann Phys Chem (Leipzig) 7:271–292
14. Landau LD, Lifshitz EM (1987) Course of theoretical physics: fluid mechanics. Pergamon, New York, 552 pp
15. Zilitinkevich SS (1972) On the determination of the hight of the Ekman boundary layer. Bound Layer Meteorol 3:141–145. doi:10.1007/BF02033914
16. Hauf T, Höller H (1987) Entropy and potential Temperature. J. Atm Sci 44:2887–2901. doi:10.1175/1520-0469(1987)044<2887:EAPT>2.0.CO;2
17. L'vov VS, Rudenko O (2008) Equations of motion and conservation laws in a theory of stably stratified turbulence. Physica Scripta T132, to be published; also: arXiv:0803.2627v1 [physics.flu-dyn]
18. Hunt JCR, Stretch DD, Britter RE (1988) Length scales in stably stratified turbulent flows and their use in turbulence models. In: Puttock JS (ed) Proceedings of I.M.A. conference on "stably stratified flow and dense gas dispersion". Clarendon Press, pp 285–322

19. Schumann U, Gerz T (1995) Turbulent mixing in stably stratified shear flows. J Appl Meteorol 34:33–48. doi:10.1175/1520-0450(1995)034<0033:TMISSS>2.0.CO;2
20. Hanazaki H, Hunt JCR (2004) Structure of unsteady stably stratified turbulence with mean shear. J Fluid Mech 507:1–42. doi:10.1017/S0022112004007888
21. Keller K, Van Atta CW (2000) An experimental investigation of the vertical temperature structure of homogeneous stratified shear turbulence. J Fluid Mech 425:1–29
22. Stretch DD, Rottman JW, Nomura KK, Venayagamoorthy SK (2001) Transient mixing events in stably stratified turbulence. In: 14th Australasian fluid mechanics conference, Adelaide, Australia, 10–14 December 2001
23. Elperin T, Kleeorin N, Rogachevskii I, Zilitinkevich S, (2002) Formation of large-scale semiorganized structures in turbulent convection. Phys Rev E 66:066305. doi:10.1103/PhysRevE.66.066305
24. Cheng Y, Canuto VM, Howard AM (2002) An improved model for the turbulent PBL. J Atm Sci 59: 1550–1565. doi:10.1175/1520-0469(2002)059<1550:AIMFTT>2.0.CO;2
25. Rehmann CR, Hwang JH (2005) Small-scale structure of strongly stratified turbulence. J Phys Oceanogr 32:154–164. doi:10.1175/JPO-2676.1
26. Pope SB (2001) Turbulent flows. Cambridge University Press, 771 pp
27. Rotta JC (1951) Statistische theorie nichthomogener turbulenz. Z Physik 129:547–572. doi:10.1007/BF01330059
28. L'vov VS, Pomyalov A, Procaccia I, Zilitinkevich SS (2006) Phenomenology of wall bounded Newtonian turbulence. Phys Rev E 73:016303. doi:10.1103/PhysRevE.73.016303
29. L'vov VS, Procaccia I, Rudenko O (2006) Analytic model of the universal structure of turbulent boundary layers. JETP Lett 84:67–73. doi:10.1134/S0021364006140049
30. Kolmogorov AN (1941) Energy dissipation in locally isotropic turbulence. Doklady AN SSSR 32(1):19–21
31. Monin AS, Obukhov AM (1954) Main characteristics of the turbulent mixing in the atmospheric surface layer. Trudy Geophys Inst AN SSSR 24(151):153–187
32. L'vov VS, Procaccia I, Rudenko O (2008) Universal model of finite reynolds number turbulent flow in channels and pipes. Phys Rev Lett 100:054504. doi:10.1103/PhysRevLett.100.054504
33. Beare RJ, Macvean MK, Holtslag AAM, Cuxart J, Esau I, Golaz J-C, Jimenez MA, Khairoutdinov M, Kosovic B, Lewellen D, Lund TS, Lundquist JK, Mccabe A, Moene AF, Noh Y, Raasch S, Sullivan P (2006) An intercomparison of large-eddy simulations of the stable boundary layer. Bound Layer Meteorol 118:247–272. doi:10.1007/s10546-004-2820-6
34. Basu S, Porté-agel F, Foufoula-Georgiou E, Vinuesa J-F, Pahlow M (2006) Revising the local scaling hypothesis in stably stratified atmospheric boundary-layer turbulence: an integration of field and laboratory measurements with large-eddy simulations. Bound Layer Meteorol 119:473–500. doi:10.1007/s10546-005-9036-2
35. Zilitinkevich SS, Esau I (2007) Similarity theory and calculation of turbulent fluxes at the surface for the stably stratified atmospheric boundary layer. Bound Layer Meteorol 125:193–205. doi:10.1007/s10546-007-9187-4